OPTICAL SWITCHING AND ITS APPLICATION IN SONET-BASED TRANSMISSION SYSTEMS

by

Philip Edward Tohme

Thesis submitted to the Faculty of the

Virginia Polytechnic Institute and State University

in partial fulfillment of the requirements for the degree of

Master of Science

in

Electrical Engineering

Approved

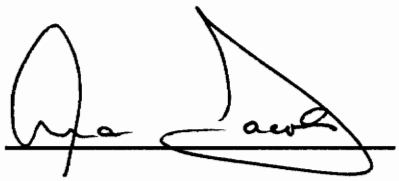

Ira Jacobs, Chairman

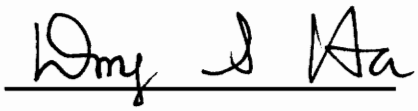

Dong Sam Ha

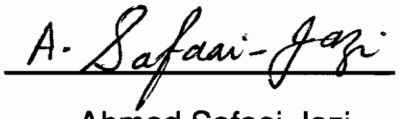

Ahmad Safaai-Jazi

September 1991

Blacksburg, Virginia

OPTICAL SWITCHING AND ITS APPLICATION IN SONET BASED TRANSMISSION SYSTEMS

by

Philip Edward Tohme

Ira Jacobs, Chairman

Electrical Engineering

(ABSTRACT)

This thesis is mainly a survey of optical devices used in optical logic and optical space, time and frequency division switching. These are mainly optical logic devices, optical switches, optical switching matrices, optical memories and optical wavelength multiplexers and demultiplexers and optical wavelength shifters. The devices are based on a variety of operating principles and are implemented with a variety of technologies. The basic principles and technologies are described together with typical performance parameters. The different devices and technologies are compared, and areas of possible improvements indicated. As an application of this survey, the possibility of implementing optical logic circuits and an optical time-division switch for Sonet based transmission systems is discussed.

ACKNOWLEDGEMENTS

I would like to thank all the people who helped me all through my masters degree, especially Dr Jacobs, Dr Ha and my brother. A special thanks to all my family.

TABLE OF CONTENTS

LIST OF FIGURES AND TABLES

1.0 INTRODUCTION

Early transmission systems consisted of electrical signals and mechanical switching. Later on, electronic switching was introduced adding to the connection speed, capacity and performance. Lightwave technology revolutionized the communication networks, offering a large bandwidth at low loss and cost. Consequently, transmission rates are nearly doubling each year, reaching 2.48 Gbps in Sonet (a recently adopted format for digital telecommunication networks) with rates such as 4.97 Gbps and 9.95 Gbps under study. Electronic switching is able to handle the 2.48 Gbps but uncertainty prevails for higher rates. Optical switching, the subject of this thesis, is seen as the next switching generation. Today's integrated optical technology is summarized and compared, followed by a study of optical switching in Sonet-based transmission systems.

Optical switching is a general term that can be interpreted in different ways. The "optical" adjective is self explanatory, it means that an optical signal is maintained in optical form all through the switching operation; that is, no optical to electrical conversion is needed.

Switching in networks may be either packet switching, circuit switching or facility switching. Packet and circuit switchings are network protocols. Circuit switching is where two subscribers are connected by a single dedicated path all through the connection. Packet switching does not contain any dedicated path, rather all transmitted data slots (packets) have their destination address as

header and it is up to the network element to choose the best path for them. Facility switching is used for protection switching where all the traffic on a failed transmission line is switched to a stand-by line for as long as the failure persists. It may also be used for network reconfiguration when traffic patterns change. Sonet is a transport format. It can support all three types of switching.

The meaning of switching in this thesis refers to lower levels of switching which considers signals primarily at the physical layer. The concerned switching techniques are space, time, and frequency division switching. Space switching is the routing of data from one physical line to another. Time division switching is where data interchanges time slots in a time multiplexed signal. Similarly frequency division switching is the wavelength interchange in a wavelength multiplexed signal. Combinations of these switching techniques may be used to achieve larger switching capacity.

The emphasis of this thesis is studying today's optical technology that is concerned with optical space, time and frequency division switching, in addition to investigating optical switching in Sonet based transmission systems. Sonet employs byte multiplexing. To access any of the Sonet multiplexed signals, overhead processing through optical logic is required. Primarily, the purpose is to determine the start, duration, and validity of the signal.

There are six chapters following this introduction. Chapter two describes the elementary optical switches which are the the basic devices in optical space division switching. An optical switch is generally (2*2), but it might as well be

(1*2) or (1*1). In a (2*2) or (1*2), an input signal is routed to either or both outputs. The switch structure generally consists of two waveguides. There are several principles and technologies on which switching light between the waveguides might be based. This results in different types of optical switches with a variety of performances. A (1*1) optical switch is an on-off device that may be implemented with a semiconductor laser diode that either passes or blocks the input signal. The material of chapter two includes a description of the basic principles and technologies of optical switches, provides representative examples and a comparison of performance.

Chapter three concerns optical switching matrices. A switching matrix is made up of elementary optical switches interconnected by waveguides to form different (N*M) architectures. Typically, any of the N inputs can form a path to any of the M outputs by controlling the appropriate elementary switches. Since each individual optical switch has some crosstalk, loss and size, these add up and generally results in optical switching matrices with low output signal to noise ratio, large signal attenuation and dimensions larger than the available substrates. To overcome these difficulties, techniques that minimize crosstalk and increase integration levels will be described. Losses can be eliminated by using devices with gain (e.g the (1*1) laser diode amplifiers) in several available architectures which will be included and compared.

Chapter four concerns optical time division switching. In a time slot interchanger, an incoming time multiplexed signal is demultiplexed into its individual time slots by a space division matrix. The time slots are then stored in

memories and rearranged to appear in a new order at the output. The main optical devices needed besides optical switching matrices are optical memories. The different types of available optical memories along with their operation principles and performance will be described. Then, several possible architectures for the optical time slot interchanger will be presented and compared.

Chapter five contains a description and performance comparison for the individual devices that make up an optical wavelength interchanger. In a wavelength interchanger, an incoming wavelength multiplexed signal is demultiplexed, each input wavelength is then shifted to its desired output wavelength, and a wavelength multiplexer forms the outgoing signal. The primary devices are thus optical wavelength multiplexers, demultiplexers and shifters. There are many types for each optical device with a wide range of performances. The chapter concludes with a description of the effect of "Four-Wave-Mixing" which contributes to crosstalk in wavelength multiplexed systems.

Chapter six concerns optical logic, where integrated optic devices that performs the normal logical operations (AND,NOR....) are described and their performances compared. The technique used to obtain several logical operations from a single optical device is described as well as derivative devices that achieve high degrees of stability.

Chapter seven discusses optical switching in Sonet based transmission systems. It is basically made up of two sections. The first consists of a Sonet

description which includes mainly its history, basic rates, format, overhead functions, and current electronic technology used for its implementations. In the second section, which constitutes the principal original work in this thesis, the implementation of optical technology in Sonet switching is investigated. An optical logical circuit that implements optical framing is analyzed. Then, the possibility of implementing optical memories in a shift register architecture for the purpose of scrambling optical signals is studied. Also, possible architectures for a Sonet-based optical time slot interchange. The chapter is concluded with some general comments on the application of optical technology.

2.0 OPTICAL SWITCHES

In this chapter, the principles, technologies and performance of (2*2) optical switches are studied. The basic operation principles are mode coupling, mode interference, and reflection from a refractive index interface. The main technologies are electro-optics, carrier injection in semiconductors, thermo-optics, all-optical, acousto-optics and magneto-optics. Based on these principles and technologies, six representative switch types are described along with a bulk magneto-optic switch and a (1*1) ON-OFF amplifier switch. The performance analysis consists of five parts. First the performance parameters are identified, these are primarily wavelength and polarization sensitivity, length, speed, power requirements, loss and crosstalk. Then a discussion is presented for the relation between different performance parameters and how they are expected to differ among the several principles and technologies. Thirdly, typical results are shown, followed by two approaches that are used to counter the polarization dependency of the electro-optic technology. Finally, long term operation stability of optical switches and other concerns are discussed.

2.1 Basic Principles and Technologies

All the above switch types except the acousto-optical and the laser diodes shares generally the same switching principles which are mainly based on mode coupling, mode interference or reflection from a refractive index interface.

Mode coupling is the transfer of energy between the modes of two coupled single mode waveguides. Every coupling length L_C, the energy totally crosses over to the opposite waveguide. The coupler switch is generally implemented with a coupling distance L equal to a single coupling length, so the switch crossover state is the default. The bar or straight through state is achieved by introducing an index of refraction difference (ΔN) between the originally phase matched waveguides such that [1]:

$$(2m)^2 = \left(\frac{L}{L_C}\right)^2 + \left(\frac{L\,\Delta\beta}{\Pi}\right)^2 \qquad (2\text{-}1)$$

where $$\Delta\beta = \frac{2\,\Pi}{\lambda}\,\Delta N \qquad (2\text{-}2)$$

is the difference in the phase constant of the two waveguides, m is an integer, L is the length of the waveguides in the coupling region, L_C is the theoretical coupling length.

From (2-1), observe that if L is not equal to L_C, $\Delta\beta$ can be tuned so that the bar state can always be achieved. For the cross state, no voltage is applied and

complete crossover depends on the exact matching of L to L_C. Implementation offsets are inevitable and cannot be countered by voltage control since L_C is voltage independent. The primary solution is in the use of $\Delta\beta$ reversal technique. This is discussed in section 2.2.1.

Mode interference differs from mode coupling in that no energy transfer exists between modes. The previous coupled waveguides are now merged in most applications. The bar or crossover state depends mainly on the relative phase difference, $\Delta\phi$, between the two orthogonal modes at the end of the single intermediate waveguide. These modes have different propagation constants which are altered generally by different amounts upon the application of the electric field (in electro-optics applications).

Note that

$$\Delta\phi = L\,\Delta\beta \qquad (2\text{-}3)$$

For the generic symmetric coupler, the equations are [2] :

$$P(\text{bar}) = 2\,A_S\,A_a\cos^2\left(\frac{\Delta\phi}{2}\right) + \left(\frac{A_S - A_a}{2}\right)^2 \qquad (2\text{-}4)$$

$$P(\text{cross}) = 2\,A_S\,A_a\sin^2\left(\frac{\Delta\phi}{2}\right) + \left(\frac{A_S - A_a}{2}\right)^2 \qquad (2\text{-}5)$$

where P(bar) is the output power from the initial waveguide (bar state), P(cross) is the output power from the adjacent waveguide (cross state), A_S and A_a are the relative amplitudes of the two modes, "s" stands for symmetric, "a" for antisymmetric, and $\Delta\phi$ is the phase difference between the two modes at the

end of interacting region.

The total internal reflection principle is based upon creating a refractive index interface in the path of the input light when the cross state is desired as shown in Figure 3. The waveguides are crossed and the index barrier is introduced in the intersecting region. Light will then be incident from a region of high index to a region of low index. For an incident angle greater or equal to the critical angle, light is reflected from the bar to the cross state. The sine of the critical angle equals the ratio of the low to high refractive indeces. This is a mode independent switching operation; consequently multimode waveguides can be used.

All these principles require the ability to control the effective index of refraction of the waveguides. Each technology has its own means to do so. Electro-optical switches alters ΔN through the application of an electric field perpendicular to the waveguides [3]

$$\Delta N = \frac{N^3 r E}{2} \qquad (2\text{-}6)$$

where r is the electro-optic coefficient, E is the electric field and N is the effective index of refraction. The electric field is generated by an applied voltage to two electrodes placed generally above the waveguides. Carrier injection switches are generally implemented in semiconductors, so an applied voltage results in a current that alters ΔN through the band filling and plasma effects. These effects are the result of light absorption by the free carriers; equations (2-17), (2-18) and (2-19) show the various parameters. Thermo-optic switches rely on the

effective index temperature coefficient. In magneto-optic switches, magnetic fields causes the effective index change. All-optical switches are generally implemented in nonlinear substrates where the refractive index is a function of the light intensity.

Semiconductor laser diode amplifiers act as on-off switches through the control of the laser bias current. Note that these switches employ optical to electrical conversion. To obtain an amplifier, the laser facets are antireflection coated to prevent oscillation. Acousto-optic switches are based on the interaction between the light signal and a generated ultrasonic wave, resulting in light diffraction. The diffraction angle depends on both the light and the sound wavelengths and the diffracted light frequency is shifted by that of the sound one. Acousto-optic switches are evaluated in the optical frequency division switching section (section 5.2) since they are mainly used as wavelength shifters.

2.2 Examples of Optical Switches

The examples that have been chosen include :

-An electro-optic $\Delta\beta$ reversal switch that overcomes the L=Lc condition in mode coupling.

-An all-optical switch based on mode coupling .

-An electro-optic X-switch that represents an application in mode interference .

-Mach-Zehnder interferometer whose technique is analogous to mode interference.

-A total internal reflection carrier injection switch.

-A thermo-optic total internal reflection switch.

-A bulk magneto-optic switch based on light diffraction from a magnetic material.

-A laser diode amplifier switch.

2.2.1 Δß Reversal Directional Coupler Optical Switch

This switch is equivalent to the normal directional coupler with the addition that both states of the switch can be attained irrespective of the matching between L and L_C. The idea is that of introducing two or more sets of electrodes instead of one and providing alternating voltage polarities. The principle can be seen in the analytic expressions of mode coupling [1] that governs the energy transfer between the two waveguides.

With a single set of electrodes;

$$\begin{pmatrix} R \\ S \end{pmatrix} = \begin{pmatrix} A_1 & -jB_1 \\ -jB_1^* & A_1^* \end{pmatrix} \begin{pmatrix} R_0 \\ S_0 \end{pmatrix} \qquad (2\text{-}7)$$

$$A_1 = \cos Z \sqrt{k^2 + \delta^2} + \frac{j\,\delta\,\sin Z \sqrt{k^2 + \delta^2}}{\sqrt{k^2 + \delta^2}} \qquad (2\text{-}8)$$

$$B_1 = \frac{k \sin Z \sqrt{k^2 + \delta^2}}{\sqrt{k^2 + \delta^2}} \qquad (2\text{-}9)$$

where (R_0,S_0) and (R,S) are the input and output amplitudes, k is the coupling coefficient, $\delta = \frac{\Delta\beta}{2}$, and Z=L.

The cross state is attained when $A_1=0$, which yields;

$$L\,\Delta\beta = 0 \quad \text{and} \quad \frac{L}{L_C} = 2m+1, \quad m \text{ is an integer.}$$

Therefore complete crossover requires V=0 and L to be an odd multiple of L_C. In the case of two electrode structures with opposite polarities, one has:

$$\begin{pmatrix} R \\ S \end{pmatrix} = \begin{pmatrix} A_1^* & -jB_1 \\ -jB_1^* & A_1 \end{pmatrix} \begin{pmatrix} A_1 & -jB_1 \\ -jB_1^* & A_1^* \end{pmatrix} \begin{pmatrix} R_0 \\ S_0 \end{pmatrix} \qquad (2\text{-}10)$$

The cross state is attained when $1\text{-}2B_1^2 = 0$, this gives according to (2-9) and with Z=L/2 :

$$\frac{k^2}{k^2 + \delta^2} \sin^2 \frac{L\sqrt{k^2 + \delta^2}}{2} = \frac{1}{2} = \sin^2 \frac{\Pi}{4} \qquad (2\text{-}11)$$

The above equation is shown in the switching diagram, figure 1 [1], as a family of curves joining two cross symbols. For the coupler to be in the cross or bar state, its operating point should fall on a curve joining two crosses (×) or two equal symbols (=) respectively. The y-axis value is (L/L_C), it is fixed for a given implementation. Tuning to the desired curve is done by properly adjusting the desired x-axis value which is the applied voltage.

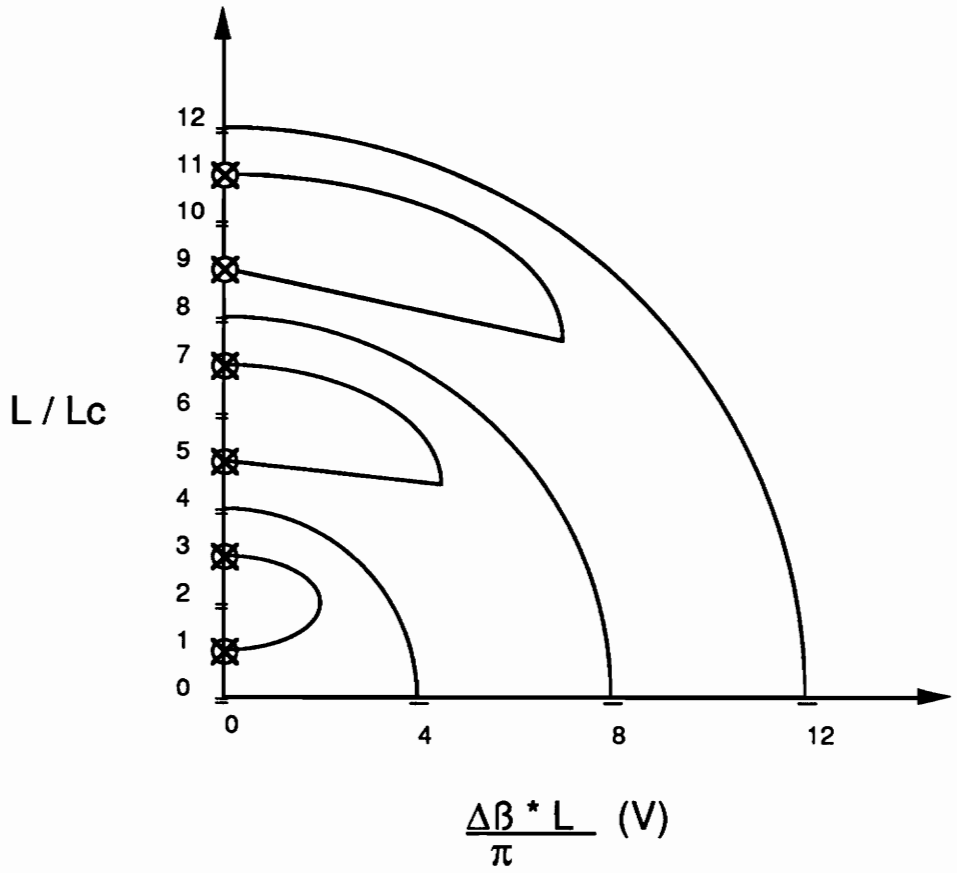

Figure 1 [1]

Switching Diagram for a Two-Section

Alternating Δß Directional Coupler

2.2.2 All-Optical Switches

The all-optical switch that is based on mode coupling is mainly a coupler implemented in a nonlinear material such as fused quartz and it is referred to as dual-core fiber nonlinear coupler. The refractive index of the waveguide (core) is a function of the light intensity according to

$$n = n_0 + n_2 I \qquad (2\text{-}12)$$

where n is the refractive index of the waveguide, n_0 is the original refractive index and n_2 is the nonlinear refractive index.

The basic operation of a typical switch is as follows : at low input powers, complete coupling takes place between the cores given that $L = L_C$. With the input power at the threshold power, the coupler is a 50/50 splitter.

$$P(th) = \frac{A\ \lambda}{L\ n_2} \qquad (2\text{-}13)$$

where P(th) is the threshold input power, A is the cross section area of the waveguide, and L is the measured coupling length between the waveguides [4]. For the demonstrated devices ([4],[5]), no coupling occurred when the input power exceeded approximatly 1.25 P(th), and complete crossover was maintained as long as the input power was kept below 0.5 P(th). P(th) is relatively high for the fused quartz material, having values of 30kW [5] and 850W [4] for typical 5mm and 1m devices. Other nonlinear glass materials with larger nonlinearities are desirable. The coupler has very fast rise and fall times provided by the nearly instantaneous index change. Typical t_r and t_f values are less than 100 fsec. The allowable bit rates is limited by the observable spectral and temporal broadening of the pulse that propagates through the nonlinear

coupler. This is caused primarily by self-phase modulation [6].

The drawback of this device is mainly apparent in two issues, the first is inability to switch a pulse as a single entity, that is any pulse has a certain rise and fall time and the part of the pulse whose intensity is less than the threshold will be coupled and the rest with P > P(th) will remain in the initial core. The other drawback is the large value of the threshold for a practical size implementation, which might cause optical damage and thus render the subpicosec switching unstable.

Another possible optical device is the Fabry-Perot resonator which is expected to work as a reflective or transmissive device by varying the optical length. When the optical length is an even multiple of a quarter wavelength, the incident light is transmitted and when it is an odd multiple, light is reflected [7]. The optical length can be varied by a bias beam which alters the refractive index of the nonlinear material. Such a device has been demonstrated with an on-off ratio of 10:1 at 0.1 Gbps and 1mW control power as typical values.

A second type of all-optical device that has been demonstrated is based on the optothermal effect. It consists of a nonlinear interference filter (NLIF) made up of alternate layers of high and low refractive indices. The NLIF state is either transmissive or reflective depending on the input power. The opto-thermal effect switching speed is in the microsecond range with a glass substrate [8], and in the 100 psec range with a saffire substrate [9].

2.2.3 The Electro-Optic X-Switch

This switch is based on mode interference. Its structure and mode propagation are shown in Figure 2 [10]. Light coupled into the fundamental mode of the input single mode waveguide excites the symmetric and antisymmetric modes of the two coupled input waveguides. These two modes are then converted to the lowest two modes in the intersection region. The last stage is the coupling of the fundamental modes into the output waveguides. The excitation of the symmetric and antisymmetric modes depends on the right tapered coupling of the inputs. The built-in index difference (ΔN) of the waveguide and the waveguide width and thickness should be chosen such that the two lowest order modes propagate throughout the intersection region. The intersection region is characterized by having an index difference of $2\Delta N$ caused by the implementation process. The power ratio coupled into the output waveguides is, as seen, a function of the phase difference of the modes at the end of the intersection. The oscillatory phases depends on $\Delta\beta$ which is electrically controlled.

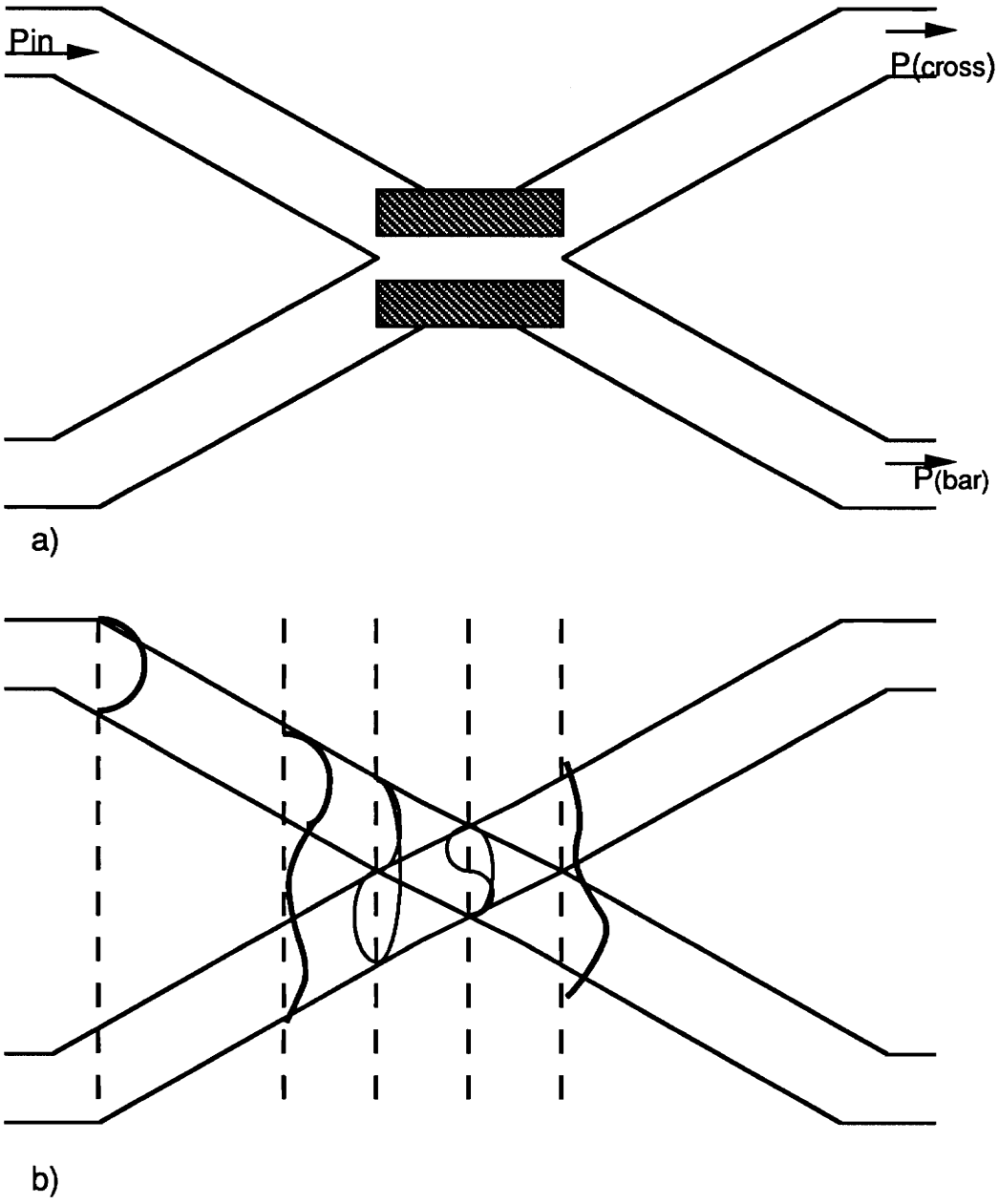

Figure 2 [10]

a) Schematic configuration of X-switch

b) Illustration of mode propagation

2.2.4 Mach-Zehnder Interferometer Switch

The switch operation follows that of mode interference achieved externally. Exciting the symmetric and anti-symmetric modes is done by introducing a 3db coupler whose outputs are connected to two single mode waveguides. To satisfy the condition of no mode coupling, the waveguides are widely separated. Introducing a relative phase difference is done by applying an electric field, in the electro-optic case, to one of the uncoupled waveguides. Then, the waveguides pass through a second 3 db coupler so that the output power distribution is solely determined by the relative phase shift. Equations (2-4) and (2-5) simplify to :

$$P(\text{bar}) = P_o \cos^2\left(\frac{\Delta\phi}{2}\right) \qquad (2\text{-}14)$$

$$P(\text{cross}) = P_o \sin^2\left(\frac{\Delta\phi}{2}\right) \qquad (2\text{-}15)$$

where P_o equals 2 A_s A_a. Using 3db couplers assures equal division of power between the waveguides, that is $A_s = A_a = 0.5$ in equations (2.4) and (2.5).

The interferometric idea, using waveguide decoupling, bypasses the exact size and doping requirements seen in the X-switch to insure no power transfer between the excited modes. On the other hand, the structure is typically a long one. It has bend and coupler losses that are not present in the X-switch for example.

2.2.5 Carrier-Injection Total Internal Reflection Optical Switch

The structure of such a device consists of a PIN structure with electrodes on the P and N side and waveguides in the intrinsic region. Carrier injection is initiated by the electrodes and is restricted to the waveguides by proper diffusion on both sides. The refractive index decrease is proportional to the injection current creating two refractive index interfaces. Increasing the current leads to a decrease in the critical angle such that when it reaches the incident angle or below, total internal reflection occurs at the first interface, Figure 3 [11]. To minimize the amount of current to be injected small injection areas are desired. Another approach to minimize the injected current is to induce a small refractive index interface in fabrication. The critical angle of the built-in interface should be much larger than all possible incident angles. Generally, scattering increases the losses of such devices and the evanescent field propagation through the index barrier adds to the crosstalk.

Another semiconductor carrier injection switch is obtained by injecting current to one of two intersecting output waveguides. With enough current, the built-in refractive index interface between the core and cladding that allows waveguiding, is eliminated. The incoming signal chooses the still valid waveguide, where the mode of the injected waveguide has been cut-off. Typical loss and crosstalk values are 3db and -20db, respectively.

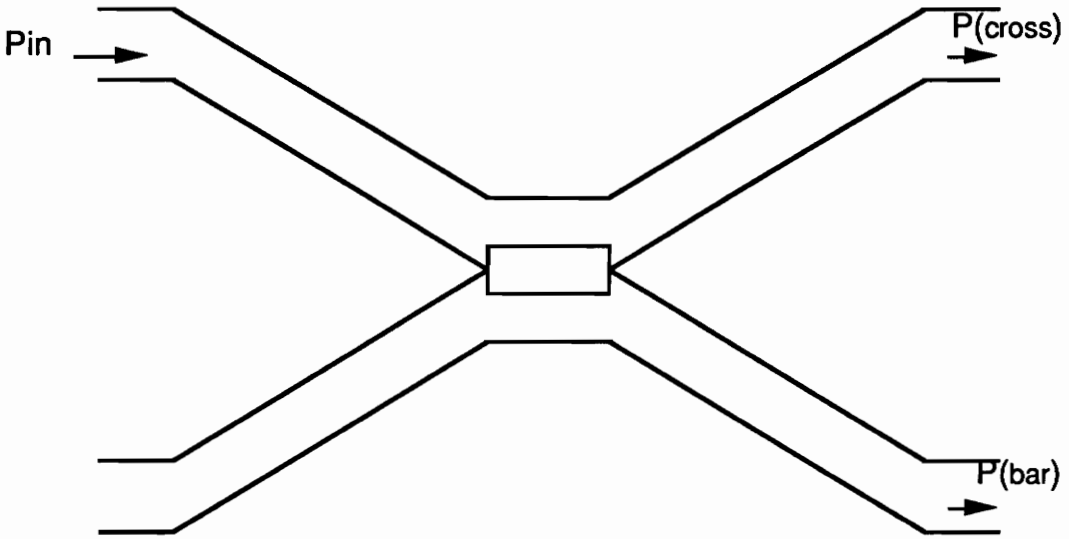

Figure 3 [11]

Schematic View of a Total

Internal Reflection Switch

2.2.6 Thermo-Optic Total Internal Reflection Switch

These switches are generally implemented in polymeric, rather than dielectric or semiconductor substrates to achieve a larger refractive index temperature coefficient. This may be seen from the following (dn/dT) values :

$-3.3 * 10^{-4}$ per deg C for polyurethane

$-1.2 * 10^{-4}$ per deg C for polycarbonate and PMMA

$4 * 10^{-5}$ per deg C for Ti:LiNbO3

10^{-5} per deg C for glass

The polymers are valid for waveguiding with refractive indices in the 1.5 vicinity, 1.49 and 1.56 for PMMA and PVR respectively. Normally, the substrate, waveguides and superstrate are all composed of polymers with different refractive indices. Heat is dissipated by applying a voltage across a very long and thin resistance placed above the waveguide intersecting region. Due to heat conduction, the temperature is highest under the heater and decreases uniformly with distance to form an index barrier of the graded type. While the thickness of that barrier is determined by the electrode spacings or the diffusion boundaries in the electro-optic and injection current cases respectively, here it is determined by the amount of heat dissipation. As the incident angle approaches the normal, a wider barrier is needed to maintain total reflection, that is higher temperatures. Polymers cannot tolerate very high temperatures, PMMA for example can tolerate a maximum temp of 95 ^{o}C before it softens. Therefore, the incident angles should be kept above a certain value by proper

switch design, otherwise the largest possible barrier may not be thick enough to cause total reflection. The rate at which thermo-optic switches can operate depends on good heat sinking where generally creating the barrier takes less time then eliminating it. Operating this switch for a long duration must take into account the variation of the heater resistance with temperature and the issue of heat accumulation. Typical performance parameters are given in Section 2.3.2.

2.2.7 Magneto-Optic Switches

Integrated magneto-optic switches that operate based on either mode coupling, mode interference or reflection are still in the early stage of research. They are faced by problems such as weak coupling, difficulty in achieving phase matching and even waveguide fabrication [12]. They are mentioned here only as an indication of their possible emergence in the future. Nevertheless the magneto-optic technology is used in implementations such as polarizers, polarizer splitters, isolators and optical storage. Bulk magneto-optic devices are also in use, they consist of light diffraction from a magnetic surface whose magnetic field orientation and strength determines the diffraction angle. An externally applied magnetic field controls the device magnetization [13].

2.2.8 A General Laser Diode Amplifier Switch

A laser diode is a one input one output switch; it either passes or blocks the input signal. It is in the ON state when the laser bias current is set very close to the threshold so that the input signal photocurrent will cause stimulated

emission. Amplification is achieved by the laser gain region. Depending on the end reflectivities, a Fabry-Perot, Traveling Wave or Near Traveling Wave amplifier is obtained. The FP amplifier (R= 0.01-0.3) has the highest gains, but its gain spectrum consists of resonating periodic peaks with narrow passbands. A large non-resonant bandwidth is provided by TW amplifier (R=0). Practically some reflectivity persists and the amplifier is a NTW .

2.3.0 Optical Switches Overall Performance

The performance of an optical switch is based on the following parameters:

-Polarization dependency

-Wavelength dependency

-The device size

-Voltage or current requirements

-Switching speed and rate

-Loss and crosstalk levels

Comparison will be made of electro-optical, carrier injection, thermo-optical and all-optical switches. This will consist of :

- Performance parameters identification and comparison
- Typical values
- Means by which the performance can be improved
- Optical technology issues

2.3.1 Performance Parameters Identification and Comparison

Polarization dependency is the case where switching differentiates between TE and TM polarizations. Polarization dependent switches are optimized to switch a single polarization. They rely on polarizers or polarization splitters and polarization maintaining fibers to provide the input. This currently translates to very high cost, high losses and complexity. If an unpolarized light is incident, the portion of power belonging to the correct polarization will be switched correctly, and the other portion might be partially switched or contribute totally to crosstalk. Normally, the input power is divided equally between the two orthogonal modes. Polarization independency is consequently a very important requirement.

Electro-optic switches generally employ rectangular geometries, and are inherently polarization dependent devices since the electro-optic coefficient seen by a TM mode differs from that seen by a TE mode. The electro-optic coefficient value depends on the substrate crystal cut and its orientation relative to the applied electric field. The difference between r(TE) and r(TM) can be minimized for certain cuts and electric field directions but generally these r values are small. This results in large switching voltages, normally greater than 100V, rendering the polarization independent switch impractical. Cylindrical waveguides are also not favored because they have weak interaction with the applied electric field due to their structure.

The electro-optic coefficient affects all switching principles. The mode coupling

and mode interference depends on $\Delta\beta$ which is proportional to r. The critical angle A_C in the reflection type is given by [14]

$$A_C = \text{Arcsin}\left(1 - 0.5\, n^2\, r\quad E\right) \qquad (2\text{-}16)$$

where E is the electric field between the electrodes, r is the electro-optic coefficient and n is the original refractive index.

Carrier injection is polarization independent since the band filling and plasma effect show no sign of being polarization dependent. This can be seen from the equations of the refractive index change; for the plasma effect [15]

$$\Delta n = \Gamma\ A(\ \lambda\ )\quad M \qquad (2\text{-}17)$$

where Γ is the optical confinement factor that takes into effect difference in distributions between the optical field and the carrier, M is the free carrier density and $A(\lambda)$ for an n-type material satisfies [16]:

$$A(\lambda) = \frac{9.6 * 10^{-21}}{n\ E^2} \qquad V^{-2}cm^{-2} \qquad (2\text{-}18)$$

where $E = \frac{h\ c}{\lambda}$ is the photon energy, n is the original index of refraction, h is Planck's constant and c is the speed of light.

Similarly for the band-filling effect, none of the factors that effect Δn is polarization dependent

$$\Delta n_{bf} = B(\lambda)\ M \qquad (2\text{-}19)$$

where $B(\ \lambda\ )$ varies as $\exp(-\lambda)$ [15].

The all-optical switch was observed to have equal coupling lengths for both polarization states, therefore one may conclude that it is a polarization independent switch.

The polymer thermo-optic switches are generally implemented in planar waveguides. Their polarization sensitivity is given by the difference between $\Delta N(TE)$ and $\Delta N(TM)$ resulting from a change in the refractive index.

$$N \Delta N = Q n \Delta n \qquad (2\text{-}20)$$

For the polymeric planar waveguides, the difference between Q(TE) and Q(TM) was less than 4%, Q(TE)=0.77 and Q(TM)=0.8 [17].

For total reflection, the minimum required index change is given by

$$\Delta N = N\left(1-\sin\theta\right) \qquad (2\text{-}21)$$

where θ is the incident angle.

Applying the voltage required to reflect the TE mode would be more than enough for the TM mode. Furthermore, the deflection angle of the two modes may vary slightly but the difference should not affect coupling to the same output fiber.

Wavelength sensitivity is mainly inherent in all optical switches. As seen previously, the means by which ΔN is achieved differs among the various technologies, nevertheless the switching indicator is $\Delta\beta = \frac{2\,\Pi\,\Delta N}{\lambda}$.

This is valid in mode coupling and mode interference. Reflection type optical switches are not expected to be wavelength dependent since their principle is based on ΔN rather than $\Delta\beta$, and ΔN may be nearly independent of wavelength.

The length of an optical switch is important because the available dielectric and semiconductor substrates are limited in size, 3" for the former and even smaller for the latter. The concern for the ability to implement large

switching matrices on the same substrate, makes the device length one of the primary factors. The length of an optical switch depends both on the switching principle and on the technology used. The latter is based on the fact that for typical applied voltages(current), the carrier injection induces refractive index change two orders of magnitude higher than the electro-optic effect, and thermo-optics refractive index change is one order of magnitude higher than the electro-optics. So in the internal reflection type, the intersecting region can be much smaller. Similarly for the mode interference, where a larger $\Delta\beta$ reaches the required π phase shift in a shorter distance. In mode coupling, the length is mainly limited by L_C which is equal to (Π / 2k), where k is the coupling coefficient. This is primarily geometry rather than material dependent so there is no preference for semiconductors or polymers.

Voltage (current) is generally dependent on the length and the required speed of the optical switch. The switching energy is usually constant, so that the switching speed is inversely proportional to the applied power. The voltage-length relation can be modeled approximatly as a VL (IL) being constant. For the mode interference, the switching condition is $\Delta\phi = \Pi$ where $\Delta\phi = L * \Delta\beta$ and $\Delta\beta$ is proportional to V so that L.V=constant. In the reflection type devices, small index change areas requires larger ΔN and hence larger voltages or currents.

Switching speed and rate are primarily equivalent in both electro-optics and carrier injection and they differ from that of thermo-optics and all-optics. In electro-optical devices, the switch can be modeled by an RC circuit where C takes into consideration mainly the capacitance between the electrodes as well

as lead and package capacitances to ground. R is mainly that of the electrodes. The RC time constant can be improved to a certain extent, by proper electrode design for example. The charging and discharging time determines the switching speed and rate. The carrier injection is also determined by its corresponding RC time constant. Thermo-optic speed and rate depends on heat diffusion and heat sinking. All optical switches speed are mainly a function of the optical nonlinear material.

Optical switches losses and crosstalk depends on the device structure and the switching principle. Total internal reflection switches introduce scattering losses due to their structure and crosstalk caused by the evanescent field propagation through the index barrier. Mode interference is theoretically a lossless operation, yet fabrication errors are inevitable. Crosstalk is introduced by voltage variation from its optimal value. Mode coupling is associated with coupling losses and incomplete coupling causes crosstalk. Waveguide propagation losses are substrate dependent. Typical ranges in db/cm are (1-3), (1-2) and (<1) for semiconductors, dielectrics and polymers respectively .

2.3.2 Typical Performance Values

Table 1 values should not be considered as limits but rather as representative values. The all-optical switch represents the fiber nonlinear coupler.

Table 1 Optical Switches Typical Performance Values

([18], [5], [19], [20], [21], [22])

	L(mm)	V,I,or power	Speed	XT(db)	Loss(db)
E-O $\Delta\beta$	3	25 V	(.1-1) ns	-25	2
All Optical	5	1.5 KW	<1 ps	--	0.1
E-0 Xswitch	2	15 V	(.1-1) ns	-23	0.1
EO Mach Zeh	38	15 V	.25-.5 ns	-20	4
C-I Reflect	1	100 mA	20 ns	-15	4
T-O Reflect	20	500 mA	1 ms	-12	1
LD Amp	1	0.3 mW	0.5 ns	-40	gain(15)

where XT stands for crosstalk which is a measure of the relative amount of power that emerges from the unintended output. Normally, the definitions are:

$$XT(db) = 10 \log_{10} \frac{P(\text{unintended output})}{P_{in}} \qquad (2\text{-}22)$$

$$\text{Loss(db)} = -10 \log_{10} \frac{P_{out}}{P_{in}} \qquad (2\text{-}23)$$

P(in) is the input signal power and P(out) is the power at the correct output.

2.3.3 Performance Improvement

The discussion of performance improvement will mainly deal with electro-optic switches. The improvement needed is in two areas :

-Overcoming the polarization dependency

-Increasing the switching speed and rate

The consideration of electro-optical switches is important because the LiNbO3 technology is the most evolved in terms of eliminating impurities and achieving homogeneity. Therefore, electro-optic switches are presently the easiest to manufacture with the largest yield .

Recall that r(TE) ≠ r(TM) which results in $\Delta\beta(TE) \neq \Delta\beta(TM)$. Polarization sensitivity can be mainly minimized in mode coupling by properly adjusting the waveguide separations all through L so that to make k(TE) = k(TM). The coupling coefficient for either mode can be approximated by [23]

$$k = k_o \exp\left(\frac{-d}{\Omega}\right) \qquad (2\text{-}24)$$

where d is the waveguide separation and Ω is the evanescent penetration depth.

k_o and Ω depend on Δn and are therefore unequal for the orthogonal modes. k_o increases with increasing Δn whereas Ω decreases. Generally, $\Delta n(TM) > \Delta n(TE)$ so that $k_o(TM) > k_o(TE)$ and $\Omega(TM) < \Omega(TE)$, but for specific d values one can obtain k(TE) = k(TM). Even with k(TE) = k(TM), the propagation

constants of the two modes are still unequal and hence their required switching voltages are different. The effect of equalizing the coupling coefficients is in minimizing the amount of crosstalk introduced when the applied voltage for a certain mode is offset from the required one. This is seen as sidelobe suppression of the switching efficiency versus voltage. Crosstalk values below -20db are attainable.

Another method to achieve polarization independent switching is to implement the electro-optic switch with two sets of electrodes, one above and one alongside the waveguides. Two electric field components would exist and therefore the phase change would have two components. For a z-cut x-propagating waveguide [24]:

$$\Delta\beta(TE) = \frac{2\Pi\, N^3}{\lambda\ 2}\left(r_{13}\, E_z + r_{22}\, E_y\right) \qquad (2\text{-}25)$$

$$\Delta\beta(TM) = \frac{2\Pi\, N^3}{\lambda\ 2}\left(r_{33}\, E_z\right) \qquad (2\text{-}26)$$

where $r_{33} \approx 3\, r_{13} \approx 10\, r_{22}$, so for the proper E_y value, polarization dependency can be eliminated.

The approach for the reflection type electro-optical switches may be that of finding a voltage and a device structure such that the critical angle of both modes is smaller than the incident angle

Improving the switching speed and rate of electro-optical switches is

mainly done by configuring the electrodes as transmission lines instead of lumped elements. This will yield subnanosec switching. Furthermore, the way the transmission lines are terminated greatly effect the settling time. The best performance is achieved by not terminating the electrodes, given that the electrodes are lossy [25].

2.3.4 Optical Technology Issues

Generally, the major concern of implementing optical switches for public use is their long term stability. The main factors that may affect the long term device operation are :

-Temperature instability

-Free carriers inside the device

-Waveguide optical damage

Long term stability of the operating voltages is a necessity if these devices are to be used commercially. Temperature variation can be countered by the use of conducting superstrates and thermal stabilizers. Optical damage is caused by large input powers, it can be avoided by keeping the input power below 20mW and 75mW for 1.3um and 1.5um respectively [26]. Protection from outside carrier surges should also be considered.

3.0 OPTICAL SWITCHING MATRICES

This chapter describes selected architectures for optical switching matrices. It starts by identifying the different performance parameters which are mainly, non-blockage, broadcasting, losses, crosstalk, integration, switch count and fault tolerance. The performance of a typical architecture usually used with electronic switches is described when implemented with optical switches. Then, the means by which performance optimization can be attained are described. These can be subdivided into three classes : crosstalk optimization using the "dilation technique", loss optimization using (1*1) laser diodes amplifier switches, and integration optimization using the "reflection technique". The chapter is concluded by describing three areas where losses can be minimized in general, these are : waveguide bends, waveguide intersections and fiber-waveguide coupling.

3.1 Optical Switching Matrices Performance Parameters

The performance of an optical switching matrix is determined by the following properties :

-Non-blockage

-Broadcasting

-Crosstalk and losses

-Integration level

-Switch count

-Fault tolerance

Non-blockage is the ability to provide any input-output connection independent from other connections. This property is sometimes relaxed to rearrangeable non-blocking, where any input-output connection is possible at the expense of the need for rearranging other already existing paths. Blockage is the inability to provide all input-output connections .

Broadcasting is the distribution of the input signal to all outputs such that the power is equally distributed.

Crosstalk and loss parameters are desired to be as low as possible. In the context of an (M*M) switching matrix, loss denotes the worst case fiber to fiber loss and the crosstalk value is generally the average of all the switching elements. Crosstalk contributes to SNR degradation and thus limits the matrix maximum allowable size. Insertion loss affects both the signal and the noise, but it may render the signal power too low for acceptable transmission. Crosstalk, in effect, is caused by individual switches and waveguide intersections. Loss is caused mainly by fiber-waveguide coupling, waveguide propagation, waveguide bends and intersections, and individual switches. Loss and crosstalk may be path dependent which result in different inputs attenuated by different amounts and output dependent SNR .

A switching matrix is said to have higher integration in the sense that its architecture allows more switches and thus larger matrix size for the same substrate area. As already mentioned, this is important since the available substrates are small and costly. The implementation of a matrix on a single

substrate is desirable but it is not a necessary condition. The advantage is the stability of monolithic devices. Most probably, the integration level would be limited. Other approaches are bonding of several substrates directly or through fiber or the use of free space connections. The latter solution would not need free space switching devices but rather classical optic devices such as lenses for focusing purposes.

Switch count represents roughly the optical switch matrix cost figure. Switch savings are generally at the expense of other performance parameter degradation such as blockage and fault tolerance .

Fault tolerance is the ability of the switch to maintain a given performance level in the presence of a single component failure. Fault tolerance is generally obtained by redundancy. For example, fault tolerance generally requires that there be more than one path for each input-output connection.

3.2 Performance of the Crossbar Matrix with Optical Switches

The optical crossbar architecture is likely the most frequently used architecture that has been translated from electronics. Its structure is shown in Figure 4 [25]. The crossbar architecture is strictly non-blocking where every input has its unique path to every output. Its broadcasting capability is not a straight forward operation, it needs precise voltage control to guarantee equal power distribution. For the 4*4 size, the first switch should have the input power split into one quarter and three quarters, the second one should have in

the bar output one quarter of the initial input power and so on, as shown in Figure 4. Note that providing the required paths for all inputs would complicate more and more the broadcasting capability.

The insertion loss is path dependent, the worst case of which is the path linking the opposite corners. For an (N*M) size, N + M -1 switches are traversed with only one in the bar state. Therefore, the worst insertion loss equals

$$IL_{worst} = IL_{bar} + (N+M-2)\, IL_{cross} \qquad (3\text{-}1)$$

where IL stands for insertion loss.

Crosstalk is also path dependent, an input signal is generally affected by noise coming from all inputs closer to the output row. For example, an input signal originating from the second furthest has noise components from the first furthest and the output row.

Generally, multiple paths are available between an input-output pair, so fault tolerance can be achieved. The number of switches needed is N*M for an (N*M) size.

The crosstalk levels of optical switches limits the maximum size of a crossbar matrix. With the value at -25 db it is limited to (6*6) given that the required output SNR is greater than 11 db and the individual switch loss is 1db. This is indicated by the dotted lines in Figure 5 [25], the worst case SNR is considered :

$$SNR_{wc}\,(db) = P(out)_N - P(noise)_N \qquad (3\text{-}2)$$

$$P(noise)_{N,i}\,(db) = P(in)_i + XT + (i+N-2)\, L_C \qquad (3\text{-}3)$$

where $P(out)_N$ is valid signal power at output N, $P(noise)_N$ is the noise power at output N, $P(noise)_{N,i}$ is the fraction of noise power at output N originating from input i, and $P(in)_i$ is the signal power at input i.

Figure 5 is obtained by mainly summing $P(noise)_{N,i}$ (watts) for every i less than N, and substituting it in (3-2).

This size limitation of the crossbar architecture reflected the need for novel optical architectures with better crosstalk capability, which came later with the "dilated networks".

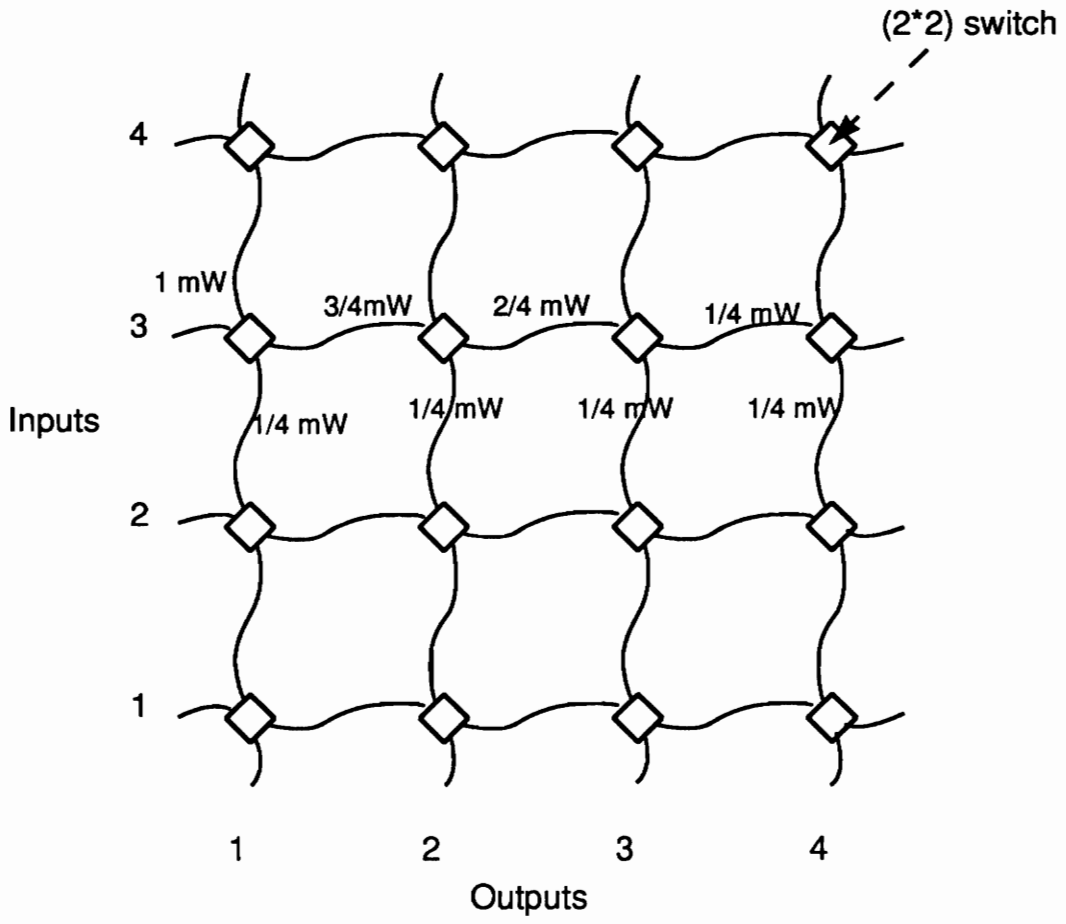

Figure 4 [25]

Crossbar Architecture

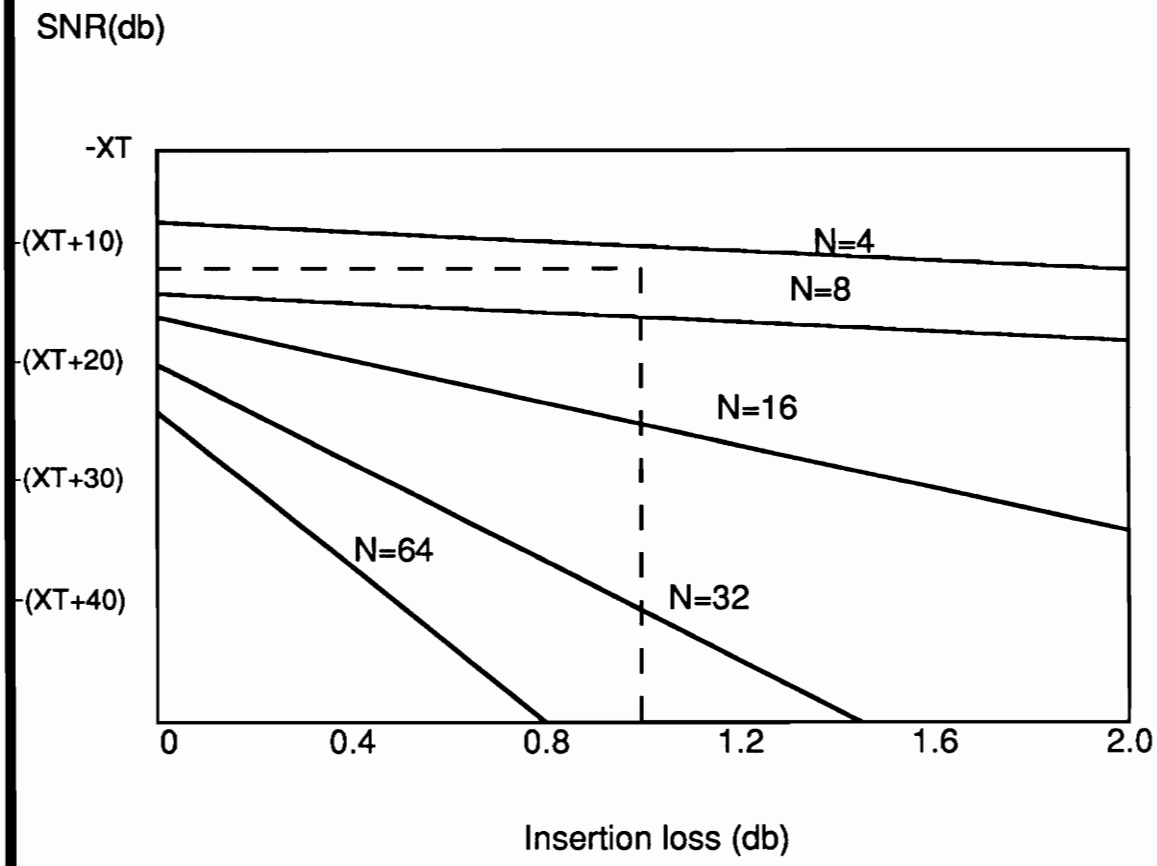

Figure 5 [25]

Crossbar Architecture Allowable Size

3.3 Low Crosstalk Optical Switching Matrices

A technique was adapted in optical switching matrices which minimizes the crosstalk of any architecture. The technique is referred to as "dilation" resulting in the so called "dilated networks". The principle is based on using only one active input in a 2*2 at any given time. The main source of crosstalk is then eliminated and only waveguide intersections, if present, will still contribute, but these contributions are generally negligible. The price to pay is a large increase in switch count which is generally more than doubled [28]. Partial dilation which allows both two and single active input switches is usually an acceptable compromise between cost and crosstalk. Figure 6 shows (4*4) Benes and Dilated Benes networks. Both matrices are rearrangeably nonblocking. The number "1" inside all switches indicates that all input output permutations can be achieved with the use of only a single input in any switch given that the correct paths are chosen.

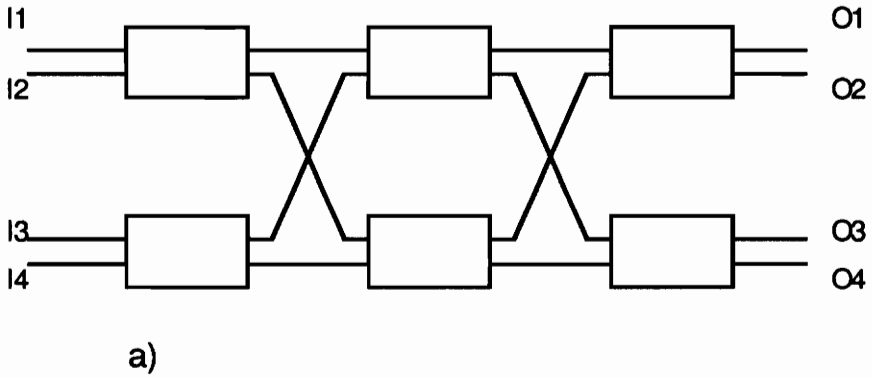

a)

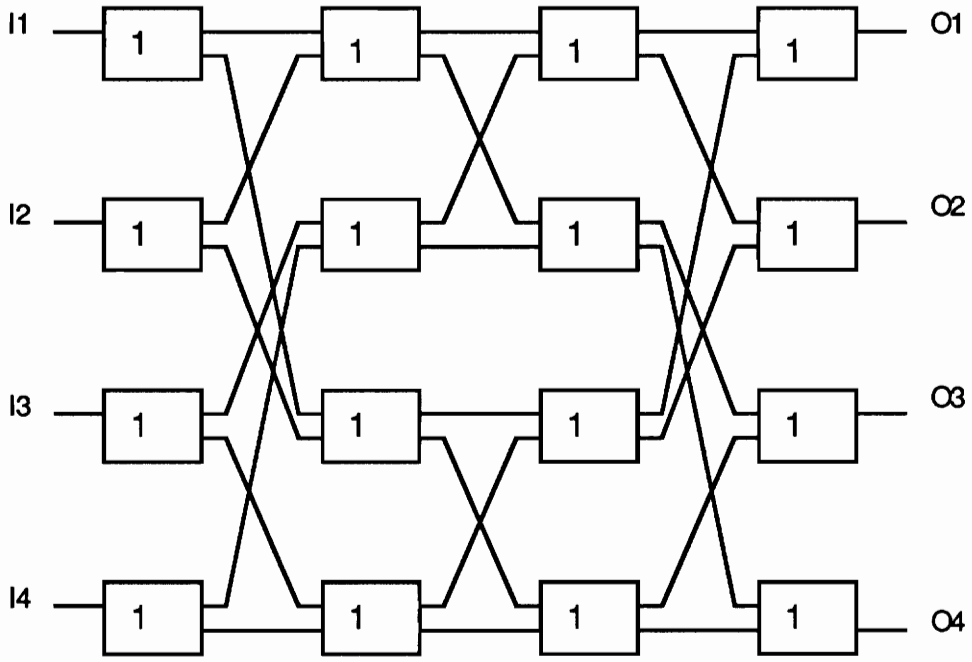

b)

Figure 6

a) (4*4) Benes Network

b) (4*4) Dilated Benes Network

3.4 Architectures and Performance of Lossless Optical Switching Matrices

These matrices have as the unit switching element a laser-diode which acts as an on-off switch through bias current control. The laser facets are antireflection coated to provide gain similar to the near traveling wave amplifier [29]. The generic architecture is shown in Figure 7a [30] for a (2*2) matrix. The input and output matrices are generally of the tree structure and the amplifier gain is set to offset the matrices losses so that the overall switching operation is lossless. The individual matrix switches can be either passive or active which results in four different configurations:

Active splitters - active combiners
Passive splitters - active combiners
Active splitters - passive combiners
Passive splitters - passive combiners

The term "passive" denotes a 50/50 splitter or combiner and the term "active" denotes a normal switch where a single input is connected to a single output. The primary differences between passive and active operations are the associated loss, crosstalk, and broadcasting properties. Studying the laser diode optical switching matrices will proceed as follows:

-laser diode tree structure general performance
-Performance based on active or passive switches
-laser diode architectures with improved performance

The tree structure architecture is totally non-blocking and fault intolerant since there is one and only one dedicated path between any input-output pair. The crosstalk, losses and broadcasting depends on matrix switches being active or passive. The switch count, for an (N*N) matrix size, is equal to 2N(N-1) which is nearly double that of the crossbar. New performance parameters introduced by laser-diodes amplifiers are the noise factor and the required gain. The noise is primarily shot and spontaneous noise. Larger matrix sizes demands larger gains that needs smaller facet reflectivities which might not be attainable. For example, a typical laser diode amplifier reflectivity had to be decreased from 0.025% to 0.006% to increase the gain by 6 db [30], such low values will be susceptible to outside reflections like interfaces, switches and bends. To overcome the required low facet reflectivities, amplification can be distributed to several amplifiers in series as will be seen later.

Passive splitters provides broadcasting capability. Crosstalk and loss values are equivalent between (passive splitters-active combiners) and (active combiners-passive splitters). Based on -20 db crosstalk, 1 db active switch and SNR >11db, the maximum allowable matrix size is (32*32) when either matrices are active and (1024*1024) for both active matrices [31]. Note that these are nearly the same constraints that imposed a maximum (6*6) crossbar size, this shows the advantage of laser diode implementations.

The only major drawback of the tree structure was the need for very low reflectivities. To overcome this constraint, one can build up a (2*2) tree

structure, that only needs amplification to offset 2 switch losses, and cascade it until the required matrix size is reached, as shown in Figure 7b. Since each unit (2*2) block is lossless, the overall structure is also lossless with minimal amplifications. Fault tolerance is provided and the other performance parameters are not degraded from the parallel tree structure if enough stages exist. The number of amplifiers needed increases from N^2 for the tree structure to 2NS for the series configuration, where S is the number of stages. Generally, the number of amplifiers are multiplied by a factor of 1.5 to 2.

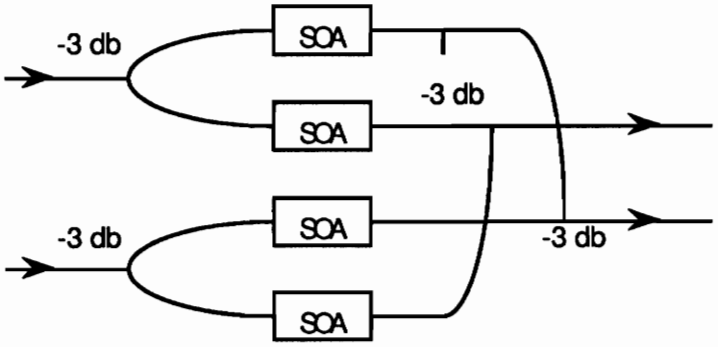

a)

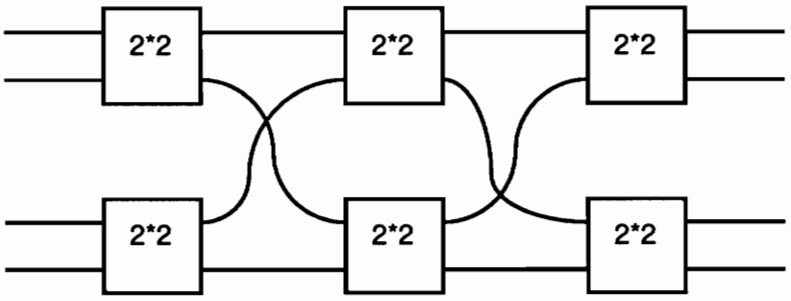

b)

Figure 7 [30]

Architectures for LD Amplifier Switch

a) 2*2 one-stage element with four

semiconductors optical amplifiers (SOA)

b) 4*4 multistage elements with 24 SOAs

3.5 Optical Switching Matrices Integration Technique

The shape of optical switches generally is that of a very large length to width ratio. Consider a directional coupler, its length is determined by the coupling length which is in the millimeter range and its width is determined by the waveguide separation and width which are in the micrometer range. The occupied substrate area is thus a small portion. The "reflection" technique is accomplished by coating one or more ends of the substrate such that the output light is reflected and passes through more switches interleaved with the initial ones.

3.6 Optical Switching Matrices General Performance Improvement

The dilation technique that minimizes crosstalk was discussed in section 3.3. Other parameters such as broadcasting, fault tolerance and switch count can rarely be changed. The waveguide intersection crosstalk can be lowered to less than -35 db if the intersection angle is made greater than 8 degrees. Optical switching matrices losses can be improved and will be discussed below. Waveguide propagation losses depend on improved fabrication where smoother surfaces and uniform doping is sought. Other loss savings can be done through better:

-waveguide intersection

-waveguide bends

-fiber-waveguide coupling

Normally waveguide intersections are implemented by crossing the two waveguides without any modification to their shape. It would be appropriate to model the propagation of light through the intersection to find the shape that causes the least disturbance, for a specific waveguide width and confinement, before implementation. The intersecting angle, width, area and shape of the intersection region may be altered accordingly. Figure 8 [32] shows a waveguide intersection whose loss (0.15 db) is a factor of two less than the normal loss.

The waveguide bends generally used are the S-shaped bends mainly due to their uniform shapes that are the easiest to implement. In the S-bends, there are many curvatures such as a sine, cosine or circular curvatures. The losses are either curvature or transition losses [33]. The transition is either a straight to curvature or curvature to curvature one in the case of two circular arc S-bend. Minimizing bend losses can be done by implementing bends such as the " coherently coupled multisection bends ". If the technology does not allow such bends, then the S-bend based on a cosine curvature should be used. A further bend loss minimization can be done by increasing specifically the bend optical confinement. Typical loss is 0.8 db/S-bend.

There are mainly two types of fiber waveguide coupling, individual fiber coupling and fiber array coupling. The former should be used if minimal losses are desired. The excess loss when using array coupling is at least 0.3 db/fiber [34]. In both cases, lower losses are achieved by better alignment and closer matching between the fiber single mode and that of the waveguide.

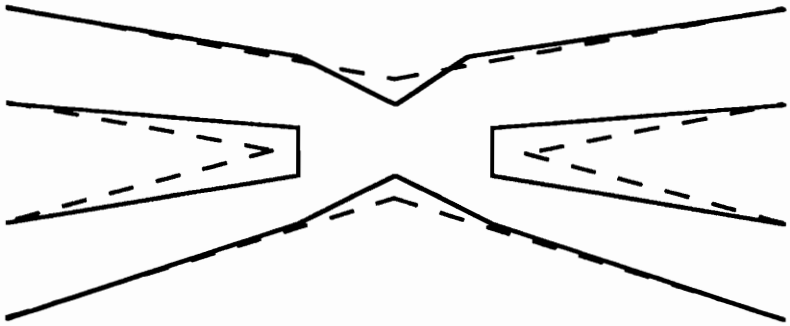

Figure 8 [32]

Low Loss Waveguide Intersection

Dotted lines : normal waveguide intersection

Plain lines : low loss waveguide intersection

4.O OPTICAL TIME DIVISION SWITCHING

This chapter describes and compares the different types of optical devices that make up an optical time slot interchanger, as well as the possible configurations of an optical time slot interchanger. The main components are optical memories and optical switching matrices that have been discussed previously. There are several possible types of optical memories such as magneto-optics, electron-trapped, laser diodes, Fabry-Perot, self-electo-optic-effect device(SEED), and optical delay lines. They are mainly based on four principles: thermal magneto-optics, electron excitation, optical bistability with hysteresis loop, and time delaying. Performance parameters of optical memories include wavelength preservation, operating wavelength, allowable bit rate and energy requirements. Optical time slot interchangers generally use delay lines as optical memories. There are four configurations, depending on whether the memories are placed in parallel or in series and whether they allow single entry or reentry. The performance parameters are switch count, switch traversals and control complexity.

4.1 Optical Memories

The first thing that should be mentioned is that optical memories are in large-scale use as compact disks for audio or video entertainment. This fact is reassuring. There are many different types of optical memories, the main ones that have an optical input and output are :

-Magneto-optic memories

-Electron-trapped memories

-Semiconductor laser diode memories

-Fabry-Perot (FP) memories

-Self-electro-optic effect device(SEED) memories

-Optical delay line memories

This chapter includes a description of the basic operation principles of these memories and a comparison of their performance.

4.1.1 Optical Memories Basic Operation Principles

The above mentioned optical memories are based on four main operation principles : thermal magneto-optics, electron-trapping, optical bistability with hysteresis loop and time delaying .

The magneto-optic storage consists of a magnetic medium, a bias magnetic field and a laser. The bias magnetic beam direction is opposite to the magnetization of the medium, yet its strength is not sufficient to cause reversal. If the laser incident data is a "1", it provides enough heat to weaken the magnetization and reversal occurs. A "0" input causes no change. Reading is done by a low power laser input which is reflected differently according to the stored data. This is a consequence of the polar magneto-optical Kerr effect where the polarization plane of the reflected light is rotated clockwise or counter-clockwise according to the medium magnetization direction. Erasing or resetting, as used in switching, is possible by reversing the bias beam direction,

which becomes that of the original medium, and applying a high power laser input. A common example is an optical compact disk implementation.

Electron-trapping storage is also an all optical read, write and reset. The principle is that of electron excitation. Writing is done by an input light pulse whose absorbed photon energy excites electrons into higher energy states where they are trapped. A "0" input energy is not large enough to cause an electron transition. Reading is done by another input beam that provides excitation energy to the trapped electrons for them to leave the trapping and fall back to their original state thus themselves emitting photons, an indication of a "1" storage. An alkaline earth crystal is usually used and the trapping levels are provided by rare earth dopants. Phosphor is used as a coating. Resetting is done in a similar fashion to reading but the supplied energy is higher (lower wavelength) to differentiate. All optical storage can also be done through atom excitation in electro-optical crystals. A high input storage alters the crystal lattice which results in a different reflection .

Optical bistability with hysteresis loop provides storage capability. Optical memories based on semiconductor laser diodes, FP and SEED devices follow this principal, but the means by which the hysteresis loop is achieved differs. FP and SEED devices will be discussed in more detail in the optical logic chapter where they form the basic logic devices. Nevertheless, both may be used for storage with optical reading and writing. SEEDs can provide resetting by voltage control; FP memories have a very short storage time of a few nanosec thus resetting is usually not needed. The semiconductor laser diode memory is

usually formed of a two gain sections and a loss section in between. It has optical inputs and outputs and the capability of either electrical or optical resetting. To demonstrate the storage principle using hysteresis loops, consider Figure 9a-b [39] that shows the operation of a laser diode memory.

Figure 9a corresponds to optical set and electrical reset. The bias current I(b) is set in between I(1) and I(2). I(1) is the threshold current above which the laser starts oscillating without input optical power. I(2) is the threshold current below which oscillation stops. The stable states are shown by the points A and C. Setting (A->B->C) is done by an optical pulse whose power is greater than P(0). Resetting (C->D->A) is done by decreasing the current beyond I(2).

Figure 9-b shows all optical operation. The stable states are shown as E and G. Setting (E->F->G) and resetting (G->H->E) are done by appropriately tuning changing the bias beam.

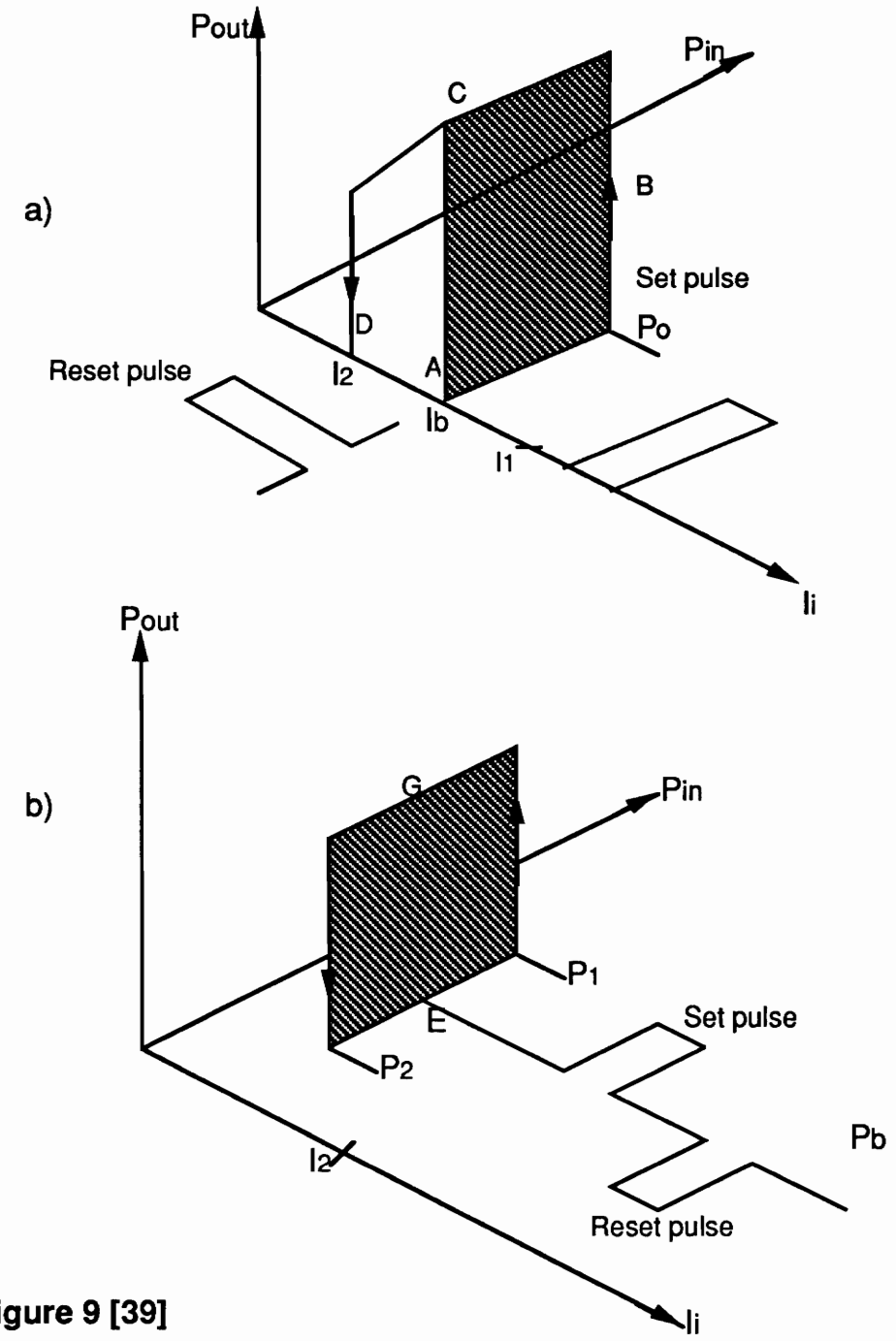

Figure 9 [39]

Bistable Laser Diode Characteristics as Optical Memory.

a) Electrical and optical control. b) All optical control.

Delay lines do not provide all of the capabilities of a general purpose memory, but do provide the capability needed in time slot-interchange. A delay line is only a usual fiber of length l. There is no read or write process but rather a light signal is directed to a delay line where it propagates and reaches the other end after l*n/c seconds, n is the refractive index of the fiber core and c is the speed of light in vacuum. In this regard, the delay line may be considered as a special kind of optical memory with a storage time of l*n/c. It is suitable for time slot interchange since the latter is based on delaying input signals by different amounts so as to rearrange their relative position. Delay lines are not general purpose memories primarily because data is not stored in the real sense and it cannot be latched at any time.

4.1.2 Optical Memories Performance

The performance parameters that evaluate a certain type of memory depend on the application. For example, audio and video optical memories should satisfy primarily two characteristics:

- Portability
- Long term storage

These parameters mainly requires a type of storage that is maintained without continuous biasing. This is found in magneto-optics and electron-trapping technologies.

Memories that are used in general transmission systems have the following main performance parameters:

- Wavelength preservation

- Operating wavelength
- Allowable bit rates
- Energy requirement

Wavelength preservation is desired since fixed wavelength receivers are normally used. If the memory does not preserve the wavelength the output wavelength should be in the proximity of the original one so that it may be shifted by optical means. Optical to electrical conversion and remodulation using a local oscillator is possible but it will add more complexity to the system. Among the described technologies, electron-trapping is the only technology that is inherently not wavelength preserving. The energy required by the electron to reach an excited state is greater than that required for it to escape to the ground state.

In contrast, delay lines are inherently wavelength preserving. Wavelength preservation for the other technologies can be satisfied if desired. The laser diode emits at a specific wavelength which may match the input one.

The SEED and FP memories have optical inputs and outputs, but the input signal does not generally form the output. This is because the input is generally absorbed and for the output to have enough power, it is formed by another signal which is referred to as the pump or probe. If the pump wavelength is adjusted to the input signal one, then wavelength preservation is satisfied.

Operating wavelength should be in the 1.3 or 1.5 um range to be consistent with the common wavelengths used for transmission.

The magneto-optic technology is based on the thermal effect therefore its

operation prefers but is not restricted to short wavelengths.

The electron-trapping technology dictates the allowable read, write, and reset wavelengths. The photon energy of the write signal should equals the difference in energies between the ground and excited state of the electron. The photon energy of the read signal should be less than that of the write one for it not to excite another ground electron but rather free an excited electron. The reset operation is similar to the read one so different wavelengths are used to differentiate both cases. Typical operating wavelengths are 0.5, 0.7, and 1.1um for the write, reset and read signals respectively. Note that this technology may not be suitable for transmission systems due to the noise introduced in resetting. The SEED memory hysteresis loop was originally shown in the viccinity of 0.85um. With specific alterations of the memory physical parameters, it was recently observed at 1.5um. The same applies for FP memories. The delay lines are wavelength independent.

The memory maximum bit rate is specified as the inverse of the minimum time needed to perform a single write, read and reset. The magneto-optic technology bit rate depends on the signal power. Large powers cause magnetization reversals more quickly.

The electron-trapping, laser diodes and SEED memories speed depend on the electrons motion, their performance is comparable to electronic memories.

The FP memory is expected to operate at THZ rates, its primary restriction is heating problems.

The delay lines are bit rate independent since they physically do not store the data.

Table 2 includes sample values that have been demonstrated and should not be taken as absolute limits since the technology is always improving.(**) denotes expected values.

Table 2 Optical Memories Typical Performance Values

	Bit rate(Mbps)	Switching power (mW)
Magneto-optic [35]	20	15
Electro-optic [36]	200	0.15
FP-memory [37]	Tbps**	0.3
SEED-memory [38]	few Gbps**	1.6
Laser-diode [39]	500	0.6

Memories to be used in a time slot interchanger are used to delay time slots by different amounts. Bits belonging to the same time slot are delayed by the same amount. Therefore, it would be adequate to have memories such as the delay lines that can store time slots as a single entity. The other technologies can only store information as bits so that a signal needs to be demultiplexed to the bit level rather than to the time slot level.

The means used to maintain optical storage can also be considered as a performance factor as mentioned earlier. The magneto-optic and electron trapping do not need any kind of biasing. The laser diode needs a constant bias

source, be it optical or electrical. The SEED and FP devices usually operates in the pulsed mode for heating considerations, therefore the biasing should also be in that form. The SEED memory can maintain storage without any biasing for a demonstrated 30 seconds. FP devices relaxes after a few nanosec.

Based on the description of the optical memories technologies and performance, one may conclude the following:
Magneto-optics is a slow and lossy technology but still is acceptable for optical disk storage.
The electron-trapping is considered an evolution compared to magneto-optics but its wavelength requirement makes it unsuitable for transmission systems.
Among the optical bistable memories, the laser diode is the most stable. For the case of optical time slot interchanger, delay lines are the best suited since they offer the required delay while preserving the wavelength, dissipating no energy and being bit rate independent.

4.2 Optical Time-Slot Configurations

A time-slot interchanger is not a general purpose switch. It is used with time multiplexed signals to interchange the position of the constituent signals. A signal that occupies say the first time-slot may be changed to the ith time-slot and so on. The purpose of the interchanging may be that individual time slots are mapped to different transmission routes or wavelengths or are left to unused traffic in subsequent space or frequency switching. In electronics, the time-slot

interchanger is VLSI implemented and it is sometimes referred to as an "elastic store". The optical time slot interchanger (OTSI) structure generally consists of an input demultiplexer, optical memories and an output multiplexer. When the unit storage of the memories is a bit, an incoming signal is demultiplexed to the bit level which are consequently routed to the memories. After all the bits are stored, the individual time slots are read out in a different order than the read to form the desired time multiplexed output.

As concluded earlier, most OTSI employ optical delay lines. These delay lines can be either placed in parallel, the usual case, or in series where demux-mux is incorporated with the delay lines. The latter form saves on switches but it has never, to my knowledge, been demonstrated mainly due to the complex switch control needed. In the parallel or series layout, different choices exist, these are :

-Parallel single entry delay lines

-Parallel reentry delay lines

-Series single entry delay lines

-Series reentry delay lines

Each individual operation will be described along with the performance which is mainly based on the switch count (cost), switch traversal (attenuation) and control complexity.

The parallel structure inherently needs demux-mux switching matrices. In the parallel reentry case shown in Figure 10, the sizes of the matrices are (1*(N/2)) and ((N/2)*1) respectively for an N time slot interchange. Each time

slot is directed to any of the delay lines since they all have the same delay D_t, this is a control advantage. D_t is equivalent to the duration of a single time slot. If a time-slot requires g delays then it has to recircle g times. The matrix controller must keep a count on each of the N delay lines which means additional control. On every reentry, the data passes through the delay line switch and is attenuated.

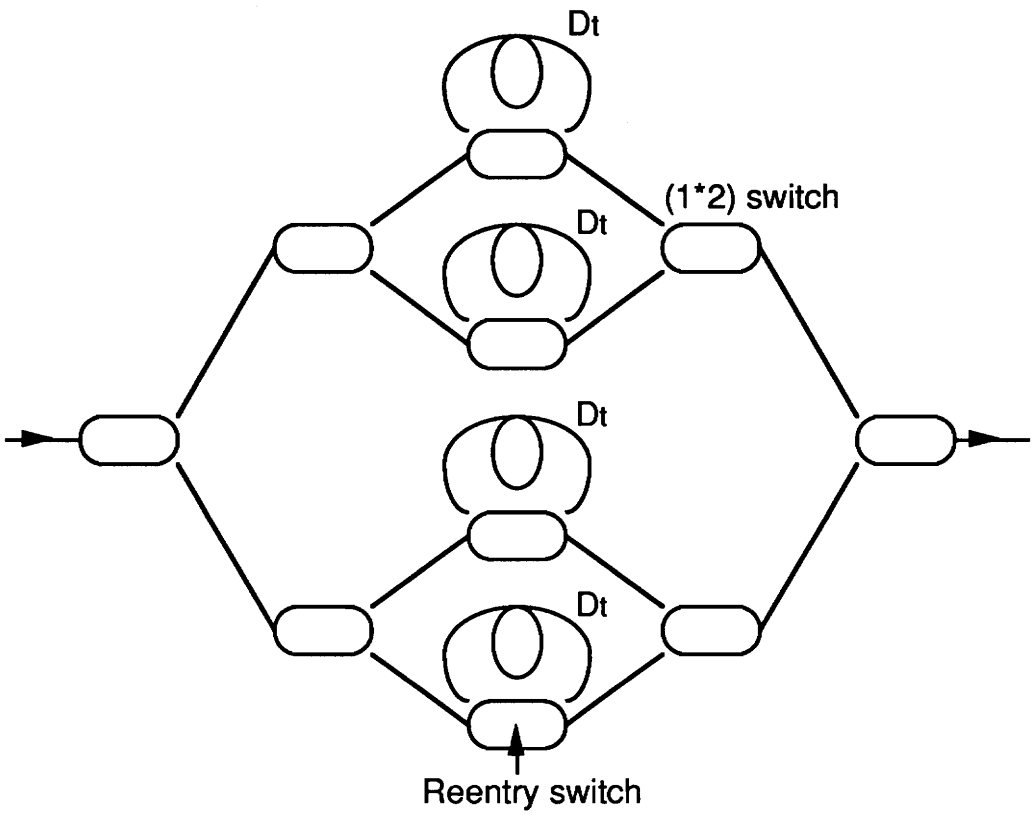

Dt is the delay of one time slot

Figure 10

Four Time-Slot Interchange Using

Parallel Reentry Delay Lines

Four time-slot interchange with parallel single entry delay lines is shown in Figure 11. A time-slot passes through a delay line a single time only. This requires a set of delay lines that offers all the necessary delays. The maximum delay is when the first time slot needs to occupy the last one in the outgoing signal, this would need a delay of $(2N-1)D_t$. So, all delays with integer multiple of D_t reaching $(2N-1)D_t$ should be provided, this amounts to 2N-1 delay lines. Since the input should be able to access every memory, (1*N) and (N*1) matrices are needed and hence more switches (cost). The major advantage is that the control algorithm does not need to keep track of any reentry count, but it has to connect every time slot to the delay line with the correct delay. Another advantage is that there are no reentry switch losses. Concluding, the parallel single entry compared to the reentry structure has:

-More switches

-Less switch traversals

-Easier control

Series delay lines do not need input-output matrices so they have a switch count advantage, offset by a more complex control compared to the parallel delay lines. A series reentry and single entry structures are shown in Figure 12 [40]. The same mentioned comparison between the parallel single entry and reentry structures are satisfied by the corresponding series delay lines. The primary characteristic of the series reentry is that the base "b" (indicated in Figure 12a) can have any integer value, larger "b" results in fewer switches.

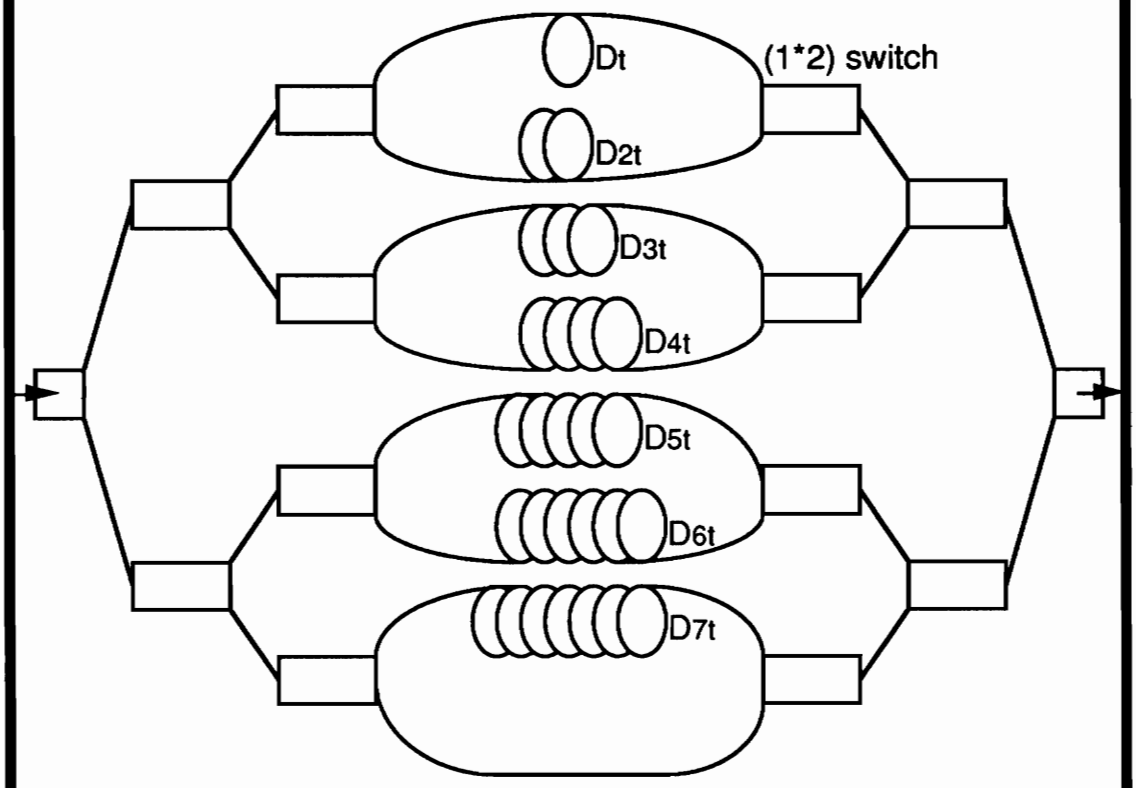

Dit is the delay of i time-slots

Figure 11

Four Time-Slot Interchange Using

Parallel Single Entry Delay Lines

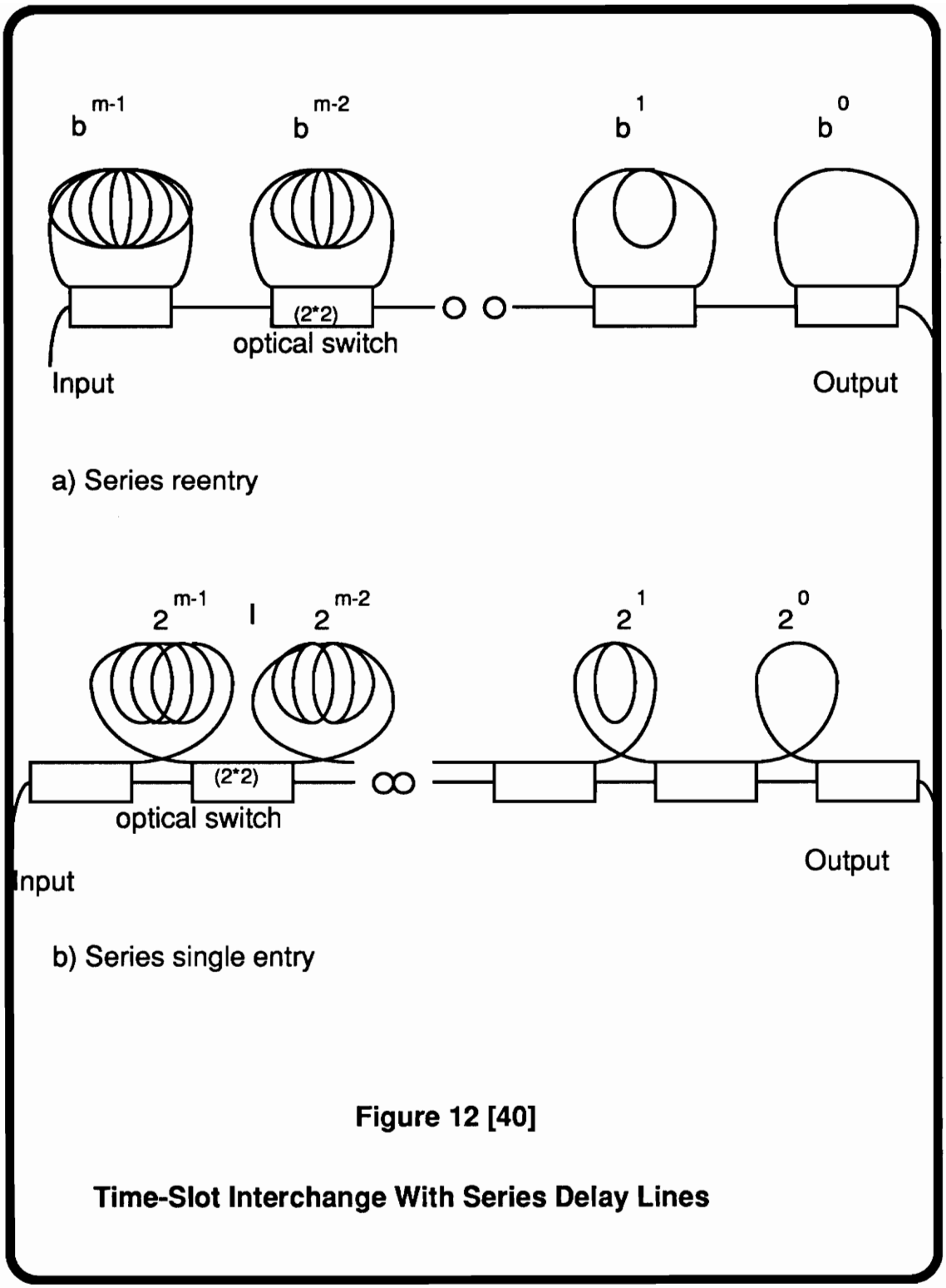

Figure 12 [40]

Time-Slot Interchange With Series Delay Lines

5.0 OPTICAL WAVELENGTH DIVISION SWITCHING

This chapter discusses and compares the different types of devices that make up an optical wavelength interchanger. These can be identified primarily as optical wavelength multiplexers, demultiplexers, and shifters. Two wavelength shifting principles are considered, acousto-optics and the use of tunable local oscillators that requires optical to electrical conversion. The main local oscillators are single longitudinal mode laser diodes (Distributed Bragg Reflectors, Distributed Feedback Lasers). The wavelength shifter performance parameters are the tuning range, tuning speed, tunable bandwidth and power requirements. Optical wavelength mux-demux types are mainly, angular dispersion devices, nonlinear interference filters, Bragg filters, Fabry=Perot filters, and optical switches using mode coupling or mode interference. Their performance is based on the allowable number of channels, required channel spacings, and expected losses and crosstalk. The chapter is concluded by describing the principle and effects of "Four-Wave-Mixing" which contributes to crosstalk in wavelength multiplexed systems.

5.1 Principle of Wavelength Shifting in Acousto-Optics

Acousto-optic switching is that of light being diffracted by an ultrasound wave. This statement may be misleading, since no direct interaction occurs, rather the sound wave alters the refractive index of the propagating medium which causes light diffraction. The refractive index change is through stress formation caused by the sound wave. There are two types of diffraction, Bragg

and Raman-Nath. The former has a single diffraction angle and the latter has many. The light wavelength is shifted with diffraction. The governing equations [41] are :

$$\sin\left(A_d\right) = m\left(\frac{\lambda}{\lambda_s}\right) \qquad (5\text{-}1)$$

$$f_d = f_o + m * f_s \qquad (5\text{-}2)$$

where A_d is the diffraction angle, m=(0,1) for Bragg and (0,+-1,+-2,...) for Raman-Nath diffraction, λ is the original light wavelength, λ_s is the ultrasound wavelength, f_d is the light frequency after diffraction, f_o is the original light frequency and f_s is the ultrasound frequency.

Bragg diffraction is usually used in frequency shifting even though the Raman-Nath provides a larger tuning range. The reason is mainly that it results in less loss. The diffraction type is indicated by the parameter:

$$Q = 2\,P\,L_i\left(\frac{\lambda}{\lambda_s^2}\right) \qquad (5\text{-}3)$$

$Q > 4\,\Pi$ => Bragg

$Q < 0.3$ => Raman-Nath

where L_i is the "light-sound" interaction length.

Note that maximum intensity is diffracted in the Bragg case when the incident angle equals the Bragg angle A_b :

$$\sin^{-1}\left(A_b\right) = \frac{\lambda}{2\,\lambda_s} \qquad (5\text{-}4)$$

The Raman-Nath diffraction is equivalent to diffraction by normal phase gratings where the gratings period is that of the sound wave. The only difference is in the induced frequency shift which is caused by the moving sound wave in contrast to the fixed grating structure. The acousto-optic Bragg diffraction does not obey the laws of normal phase gratings but rather of diffraction from a sinusoidal refractive index disturbance. The diffraction spectrum contains only two peaks corresponding to m=0 and m=1.

As mentioned, the frequency shift is attributed to the motion of the sound wave which causes a traveling index wave. It was also shown that a traveling index wave can be formed by electrical means. This is done by applying a three phase sinusoidal voltage to the electrode gratings [42]. At any fixed point, the voltage changes sinusoidally resulting in a sinusoidal index change. This is equivalent to the behavior of a traveling index wave. Electro-optic frequency shifting has higher losses and lower carrier to sideband conversion efficiency compared to acousto-optics therefore the latter technology is generally used.

5.2 Optical Wavelength Shifting Devices

An acousto-optic wavelength shift is done at the optical level. Another possible approach would be to detect the optical signal and then use the photocurrent to modulate a tunable local oscillator. The items that will be discussed are:

-Various forms for acousto-optic devices

-Available tunable local oscillators

The wavelength shifters based on acousto-optics are mainly implemented on piezoelectric substrates such as LiNbO3. The waveguides are generally crossed or planar. In the crossed case, a third waveguide with length L_i is placed above the intersection region, it is the acoustic waveguide. When there is no acoustic excitation, a light signal maintains its initial waveguide. When an ultrasound wave propagates, light is diffracted from its original path to the next waveguide.

A problem exists, equation (5-1) shows that the diffraction angle is a function of the ultrasound wavelength, therefore every desired wavelength shift has its own diffraction angle. Since the waveguides have a limited acceptance angle (numerical aperture), unacceptable losses may result. Planar waveguides overcomes this difficulty by introducing a focusing lens either inside the substrate or a bulk one, so as to couple the light into the fiber. Yet, for single mode fiber, some losses will still occur. The use of a focusing lens may not be desirable for implementation considerations. Another way to achieve an output with a fixed direction is to use two transducers with distinct frequencies in cascade, such that they are tilted with respect to each other by an angle equal to the difference between their corresponding Bragg angles. If they are tuned by the same frequency amount, the light wave which is now diffracted twice will maintain the same output direction independent of the frequency shift [43].

For the tunable local oscillators, the main monolithic types used are:

-Distributed Bragg Reflector (DBR LD)

-Distributed Feedback (DFB LD).

The DBR LD structure is made up of three sections, active, phase control and Bragg reflector. Currents are injected to all three sections. The active current determines the output power. The section and phase current controls the wavelength tuning. Single tuning may be used at the expense of a smaller tuning range. The largest tuning is when I(Bragg) equals three times I(phase). This only requires a single current source with a current divider. The DFB LD structure can be mainly one of two types, the first consists of several electrodes above a grating where the ratio of the electrode voltages determines the tuning. The second is made up of two sections, a grating and a phase control. In general, the DBR and DFB LDs are based on the same principal which is that of phase matching. For instance, in a DBR, a lasing mode satisfies:

$$\phi_1 = \phi_2 + 2m\Pi \qquad (5\text{-}5)$$

where ϕ_1 and ϕ_2 are the phase changes in the Bragg and active plus phase regions respectively.

Wavelength tuning is done by carrier injection which alters the refractive index shifting the equality in (5-5) to shorter wavelengths.

5.2.1 Performance of Wavelength-Shifting Devices

The parameters that primarily determine the performance of wavelength shifting devices are :

- Tuning range
- Tuning speed
- Power requirements

Table 3 Wavelength Shifters Typical Performance Values ([43], [44], [45], [46])

	Tuning range	Tuning speed	Power or current
DBR-LD	4.4 nm	8 ns	150 mA
DFD-LD	2.4 nm	8 ns	100 mA
A-O	<1.0 nm	2 us	200 mW

-The slow switching speed of the acoustic device is due to the low propagation speed of the ultrasound wave. It can be enhanced if the sound wave is excited prior to tuning.

-The tuning limits of the DBR-LD and DFD-LD is around 15 nm imposed by the maximum allowable current injection.

-Larger tuning ranges can be obtained by external or compound cavities for example. They can provide ranges as high as 50nm at the expense of mechanical or high voltage electrical control .

5.3 Optical Wavelength Mux-Demux and Filters

The main optical devices used are :

-Angular dispersion devices

-Nonlinear interference filters

-Bragg filters

-Fabry-Perot filters

-Switches based on mode coupling or mode interference

-Active devices

5.3.1 Basic Operations of Optical Wavelength Mux-Demux

The angular dispersive device is usually in bulk form. It mainly consists of a grating and a lens. An incident wavelength multiplexed light signal is reflected into several wavelength dependent angles. The lens function is to focus each individual wavelength to its corresponding fiber. The reverse operation would be that of an optical wavelength multiplexer.

The nonlinear interference filter (NLIF) and Bragg filters are based on nearly the same principle. The NLIF acts as a passband, it transmits a certain wavelength and reflects the others. The Bragg filters reflects the chosen wavelength and transmits the others. Wavelength filtering is based on refractive index change. The NLIF is implemented as alternate layers of high and low refractive indices, and the Bragg filter relies on electrode gratings. Wavelength

mux-demux can be constructed from filters. Every filter extracts a certain wavelength and passes the rest of the signal to another filter which will filter out another wavelength. Hence after sufficient stages, the signal is totally demultiplexed and the reverse operation would form the multiplexer. Using filters in cascade has a negative loss aspects; loss would have large values and it would be unequal for different channels.

Another type of wavelength filter is the Fabry-Perot resonator whose spectral transmission consists of a set of transmission peaks. Filtering is done by tuning one of the transmission peaks to the required wavelength. Conditions that should be satisfied are that the distance between FP transmission peaks be greater than the system spectral span and that the passband be narrow enough to minimize crosstalk. Therefore, a figure of merit referred to as "finesse" is the ratio of the spacing of the transmission peaks to their FWHM. Tuning is done by changing the optical length (nL) of the resonator where n is the refractive index and L is the distance between the mirrors.

It was shown previously that mode coupling and mode interference based optical switches are wavelength sensitive. These switches can thus be used as wavelength filters where the filtered wavelength is the one that has the required $\Delta\beta$ for switching.

Active devices are multiwavelength sources and detectors. They are generally not used mainly due to restrictions on the individual channel power and instability .

5.3.2 Performance of Optical Wavelength Mux-Demux

The primary performance factors are:

-Allowable number of channels

-Required channel spacing

-Induced crosstalk and losses

Table 4 Optical Wavelength Mux-Demux Typical Performance Values ([47], [48], [49], [50], [51])

	Channel num	Spacing(nm)	XT(db)	Loss(db)
Angular D	(3-20)	(1-40)	(-20;-30)	(1-4)
NLIF	(2-6)	(30-100)	(-20;-70)	(0.5-5)
Bragg filter	4	5	-20	3
FP filter	(2-10)	10	-20	3
Mach-Zeh	4	(5-10)	-15	2.6
Symm-cplr	<8	(30-40)	-35	<3

In an optical wavelength interchange, the wavelength shifters and mux-demux are complementary, that is the wavelength shift should be equal to the product of the channel number and separation. It was seen that typical tuning ranges of the local oscillators and acousto-optics are in the few nanosec range which is much less than what would be required given the values of table#4.

5.4 Four-Wave Mixing

In previous sections, there were mainly two factors that concerns wavelength multiplexed signals :

-Most optical switches were wavelength sensitive

-Optical damage

The optical switches wavelength sensitivity was used advantageously in optical filters. In general, it is a restricting factor to the implementation of wavelength multiplexing in optical switching.

Since the light signal power increases considerably with wavelength multiplexing, optical damage should be considered more than in single wavelength signals.

Optical switches make use of non-linearities, but non-linearities cause intermodulation products in a wavelength multiplexed signal. Main concern is the third order intermodulation which leads to effects such as intensity dependent index of refraction, optical bistability and four-wave mixing (FWM).

FWM is the process in which multiplexed frequencies generate new ones that contribute to noise. Any two or three frequencies generate a fourth one whose frequency is [52]

$$f(\text{noise}) = f(i) + f(j) - f(k) \qquad i \neq k\,,\ j \neq k \qquad (5\text{-}6)$$

where f(i), f(j), f(k) are the frequencies of laser i, j and k respectively, and f(noise) is the frequency of the generated noise.

FWM holds for unidirectional and bidirectional transmission. Systems are generally designed such that the noise generated by FWM accounts for nearly half the total noise in a receiver. Placing the channels at unequal intervals results in the generated spectrum being displaced from the signal, this decreases noise but does not eliminate it. Channels largely separated are effected less by FWM. An important issue to be considered with electro-optic wavelength filters is that the FWM noise increases by a factor of 9 with single polarized light [52]. The reason being that the noise power is a function of the third order susceptibility which is a tensor whose value apparently maximizes when the individual fields have the same polarization.

6.0 OPTICAL LOGIC

This chapter describes the operation and performance of integrated optical devices that performs logical operations. Two devices, the Fabry-Perot (FP) resonator and the Self-Electro-Optic-Effect Device(SEED) are considered. The "probe" technique which allows the implementation of any logical operation in a single nonlinear(FP) is discussed as well as the S-SEED device that achieves stable operation. Performance parameters are logic operation speed, bit rate, and energy requirements. Typical results, comments and theoretical limits are included.

6.1 Integrated-Optic Logical Devices

Optical logic generally makes use of nonlinear optical behavior. The nonlinearity is mainly achieved either by an all-optical device (FP), or through an electro-optical one (SEED). Both devices have optical inputs and outputs and the logical operation is performed with the signal maintaining its optical state.

The self electro-optic effect device has optical inputs and outputs with electronic feedback. It consists of a semiconductor multiple quantum well (MQW) embedded in the intrinsic region of a PIN diode structure. A resistance and a dc voltage source provide the feedback as shown in Figure 13a [53]. With low input power, the reversed biased PIN acting as a photodetector provides a small photocurrent to the resistor. Therefore a large voltage is

applied across the diode, which results in the shifting of the absorption spectrum towards longer wavelengths. As the input light is increased, more photocurrent results in a smaller voltage across the MQW, the absorption peaks return back to the original wavelength triggering more absorption and resulting in a reduction in the output. It is a threshold behavior that shows as a nonlinear relation between the input and output powers, Figure 13b [53].

The MQW structure is responsible for the device operation, since normally semiconductors respond to a normal electric field by a slight absorption shift and only at low temperatures (Franz-Keldysh effect). The MQW behavior is described by the Quantum Confined Stark effect which explains the phenomena on the basis of minimum ionization of the material due to the confinement of electrons and holes in the wells.

Besides the nonlinearity, the characteristic curve includes a hysteresis loop. It is due to the photodiode responsivity R (Figure 13c [53]), the solid line is the measured R(V) and the dashed lines corresponds to the R values that satisfies I=R*Pin. For the same input power (a single dashed line), two or three intersections may exist and thus two output power levels, the third level is unstable. The small hysteresis loop is due to the light exciton peak, it appears with large voltages.

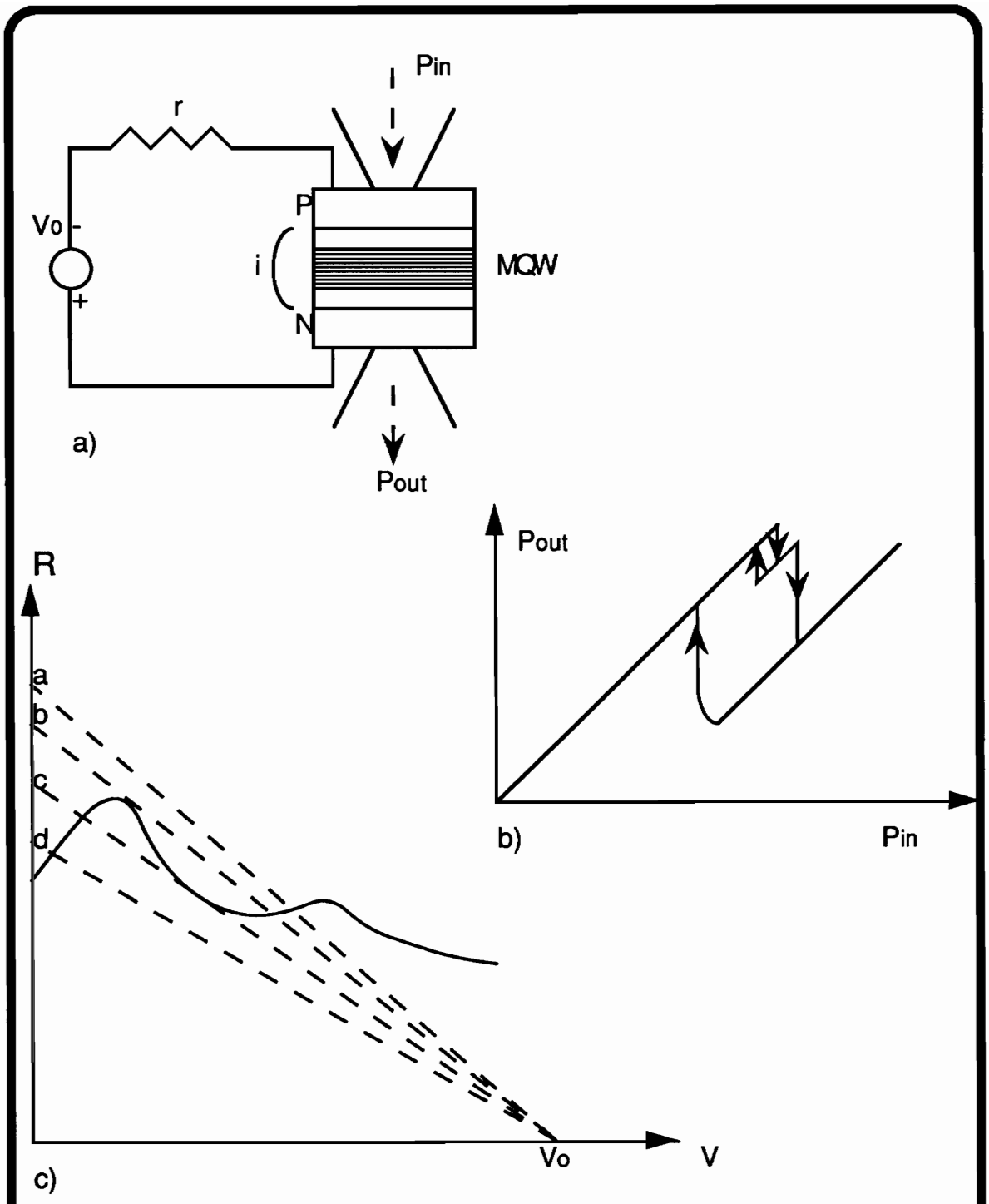

Figure 13 [53]

a) SEED Structure b) SEED Characteristic Curve
c) SEED Responsivity Curve

The nonlinear Fabry-Perot consists of a Fabry-Perot resonator made up of a nonlinear material in between two mirrors. The nonlinearity has a different shape from that of the SEED, it is a saturable absorber, Figure 14 [54]. The building up of the nonlinearity and bistability is also more involved, governed by the relations between light intensity inside the cavity and the transmission factor. Nevertheless, the operation is effected by the offset between the input wavelength and the cavity resonance which is called "detuning". If the signal wavelength coincides with the resonance, then the transmission is linear. The nonlinearity increases and the hysteresis loop widens with increased detuning. This is also due to a shift in the transmission peak with an avalanche behavior. The resonance shift is caused mainly by thermal or electronic effects. The material used can be GaAs, InSb, ZnSe, glass or others. This device is considered all-optical since it does not need a voltage or current source.

6.2 Optical Logic Operations

The logical operations make use of the nonlinear P_{out} versus P_{in} characteristic. A bias beam is applied to set the operating point very close to the nonlinearity. When the input is a logic "1", the nonlinearity is reached. This shows as a drop in the output power for the SEED (inverter) and an increase in the case of NLFP(AND). Several inputs can be used by providing enough space between the bias position and the nonlinearity, therefore SEED would represent a NOR gate.

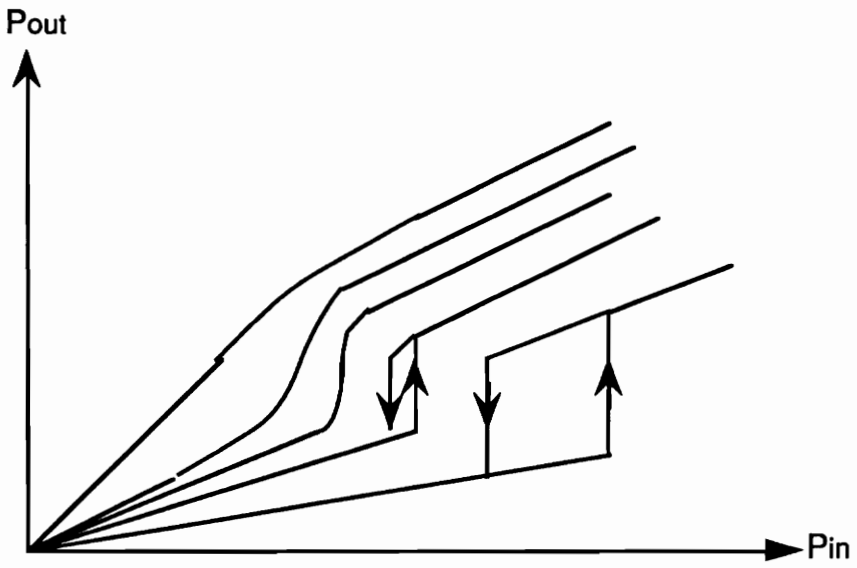

Figure 14 [54]

Family of Curves of Nonlinear Fabry-Perot

Obtained by changing the Initial Detuning

The reliability of the logic operation depends on the stability of both the bias beam and the nonlinear curve. Furthermore, the available gates are restricted to a few types. The answers to these problems came primarily with the introduction of the symmetric-SEED (S-SEED) and the demonstration of all the logical operations in a NLFP with the help of the "probe" technique.

The "probe" technique is used only with NLFP and it is based on very precise wavelength tuning. The inputs are first applied. The absorption of an input changes the refractive index of the resonator resulting in a shift in the Fabry-Perot transmission spectra. The probe is applied following the inputs and prior to the medium relaxation [55]. The various gates are obtained by properly tuning the probe wavelength which forms the output. If the probe wavelength coincides with a transmission peak, then the output is high otherwise the probe is also absorbed and the output is low.

The Symmetric-SEED (S-SEED) consists of two SEEDs placed in series between a dc voltage and ground. Its characteristic curve is similar to the SEED's with the advantage that the operating point is effected by the ratio of the two inputs. Consequently, if the same bias signal is applied to both inputs then a high degree of stability is achieved .

6.3 Logic Devices Performance

The performance parameters are mainly:

-logic operation speed

- logic operation maximum bit rate

-logic operation required energy

The SEED or S-SEED are primarily electro-optical devices that are limited by the RC time constant. The maximum rate cannot be higher than electronic devices, it might be much slower depending on the MQW characteristics. They have a constant switching energy, the same for NLFP, therefore the performance is a power speed trade-off.

The nonlinear FP is characterized by the relaxation time of the material. It is the time for the transmission peak to return to its original position after a logic operation. A relaxation constant, t_r, is defined for a nonlinear optical material where total relaxation needs a few t_r. Evidently, the relaxation constant determines the allowable operation rate. Normally it is in the range of a few nanosec; a typical value is 5 nsec, yet it can be decreased to picoseconds by doping, photon bombardment, or surface recombination [REF 56].

The "probe" technique was based on exact detuning. Since the transmission resonance is susceptible to thermal effects, the maximum rate is as well limited by device heating. In fact this is why NLFP operates in pulsed mode. The origin of the nonlinearity determines the amount of heat dissipation, evidently the

absorptive origin is the worst. In general, thermal effects should be considered when the device is operating roughly above 10GHZ [57]. In this region, the allowable rate is less than the absolute maximum provided by a given nonlinearity.

The speed of the NLFP depends on how fast the exciton transmission peak responds to excitation. It is primarily affected by the magnitude of the nonlinearity and the resonator length. The former is material dependent and the speed is inversily proportional to the length.

Table 5a Optical Logic Devices Demonstrated Performance

Table 5a	Energy (pJ)	Speed (ns)
S-SEED [58]	640	40
SEED [38]	8	30
NLFP [59]	20	0.1

Table 5b Optical Logic Devices Expected Performance

Table 5b	Speed	Energy	Power
NLFP(PTS) [57]	0.1 ps	0.1 pJ	1W
S-SEED [60]	0.3 ns	10 fJ	33 uW

7.0 OPTICAL SWITCHING IN SONET

The previous chapters described mainly the basic principles, technologies and performance of optical space, time and frequency division switching. A possible system application for these devices is the Synchronous Optical NETwork (SONET). Sonet is selected because it is the transmission format planned for future telecommunication networks. It has high transmission rates that presently reaches 2.48 Gbps and are planned to increase further to 9.95 Gbps in few years. Sonet employs time-division multiplexing. At high speed transmission, it is desired to be able to add, drop, crossconnect or interchange individual signals at the optical level.

This chapter consists mainly of two parts. First, Sonet is described. The description includes mainly its origin, format, basic rates, overhead functions and the current electronic technology used for its implementations. The second part constitutes the principal original work in this thesis. The means by which optical technology can be implemented in Sonet is studied. This will include an analysis of the following main topics:

The implementation of nonlinear Fabry-Perot logic and all-optical switches in a combinational circuit for the purpose of signal optical framing. The required performance of a NLFP gate including its speed, delay and relaxation time is investigated. The architecture consists of a cascadable structure that is capable of observing all bit sequences and thus provides systematic alignment to a Sonet frame.

The use of architectures that employs hardware duplication in order to relax the operation rate of circuits for thermal or speed reasons. The architecture may be used for optical framing and the proposed technology is high speed all-optical switches and low speed optical logic.

The use of various technologies of optical memories in a shift register architecture for optical signal scrambling.

The study of a Sonet-based time slot interchanger. Given the Sonet format, the single entry and parallel entry delay lines architecture will be compared. The Sonet-based OTSI is proposed to be made up of two separate structures, one for virtual tributary (VT) and the other for optical carrier (OC) interchange. The need to preserve the Sonet format in the interchange is considered.

7.1.0 Sonet Description

Sonet description will include a brief history, its current electronic technology, format and rates, main network elements, and overhead functions.

7.1.1 Sonet History

Sonet stands for Synchronous Optical Networks. It is a standard for fiber optic transmission for North America, its worldwide equivalent is identified as "Synchronous Digital Hierarchy" (SDH). Work on the Sonet standard started in 1984, the format and rates were finalized in 1988, and in mid 1990 most of the operation and maintenance channels standardization were published. To date there are still some minor standardization to be completed. Sonet network element deployement began in late 1989. Sonet is to replace completely all the manufacturer based incompatible asynchronous fiber optic networks, into a single robust countrywide (worldwide) network. It is mainly an interoffice high speed transmission network but it can also include the subscriber loop and even be connected directly to the home in the future. Sonet's maximum transmission rate can be increased modularly, it is currently at 2.488 Gbps and is expected to reach 9.95 Gbps in the coming few years.

7.1.2 Sonet Electronic Technology

When the Sonet rates were set in the mid 80's, there were a lot of speculations on the electronics capability to handle them. Nevertheless, the emergence of the GaAs technology solved the problem of the slow CMOS (Complementary Metal Oxide Semiconductor) and the ECL (Emitter Coupled Logic) that needs exotic cooling. GaAs is costly and its processing and integration technology is not yet evolved as that of CMOS, so low speed operations were kept for CMOS or BiCMOS (Bipolar CMOS) that have a maximum operating rate of 120 MHZ within acceptable device heating. Figure 15 [61] shows the performance of the three technologies, note that conductive cooling is generally the only acceptable one for public use switching circuits. The other main problem with electronics is that RC value which determines the device switching speed remains constant with integration. With "s" as the scaling factor, the scaled resistance is multiplied by "s" and the capacitance is divided by "s" so that their product remains unchanged.

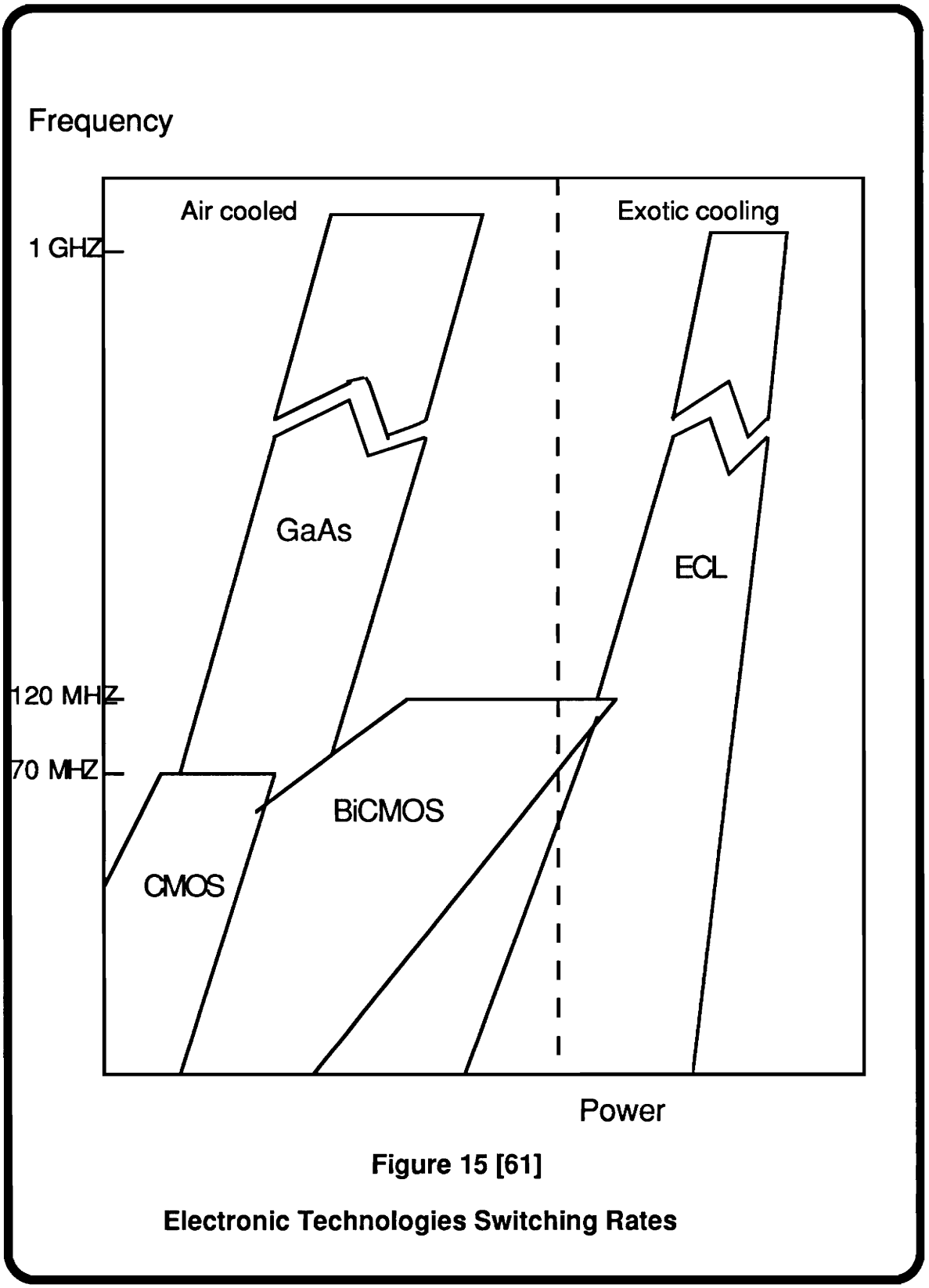

Figure 15 [61]

Electronic Technologies Switching Rates

7.1.3 Sonet Rates and Format

The basic Sonet signal is the STS-1, Synchronous Transport Signal -1, whose rate is 51.84 Mbps. Its frame is 125 usec long consisting of 9 rows and 90 columns with the single unit being a byte, Figure 16 [62]. The first three columns are reserved for the transport overhead, the fourth column is the path overhead. By byte interleaving N STS-1, an STS-N is formed whose rate is N times that of an STS-1. The transport overhead are aligned to form the first 3N columns. Note that the frame of an STS-N is also 125 usec long. The available N values are 1, 3, 9, 18, 24, 36 and 48 where 2.488 Gbps corresponds to N = 48. The values of N that are under study are 96 and 192. Signals of unit rates above 51.84 Mbps such as broadband ISDN signals are transported by concatenating several (n) STS-1 frames. The STS-nc frame would have only a single path overhead and it is treated as a single entity in switching. Rates below 51.84 Mbps are also supported to allow existing signals (e.g. T1) to be supported in Sonet. This is accomplished with virtual tributaries(VT). The supported rates are VT1.5 (1.728 Mbps), VT2 (2.304Mbps) , VT3 (3.456 Mbps) and VT6 (6.912 Mbps). Figure 17 [62] shows a frame consisting of 28 VT1.5. OC-i is the optical equivalent of the STS-i after scrambling, it stands for optical carrier level i.

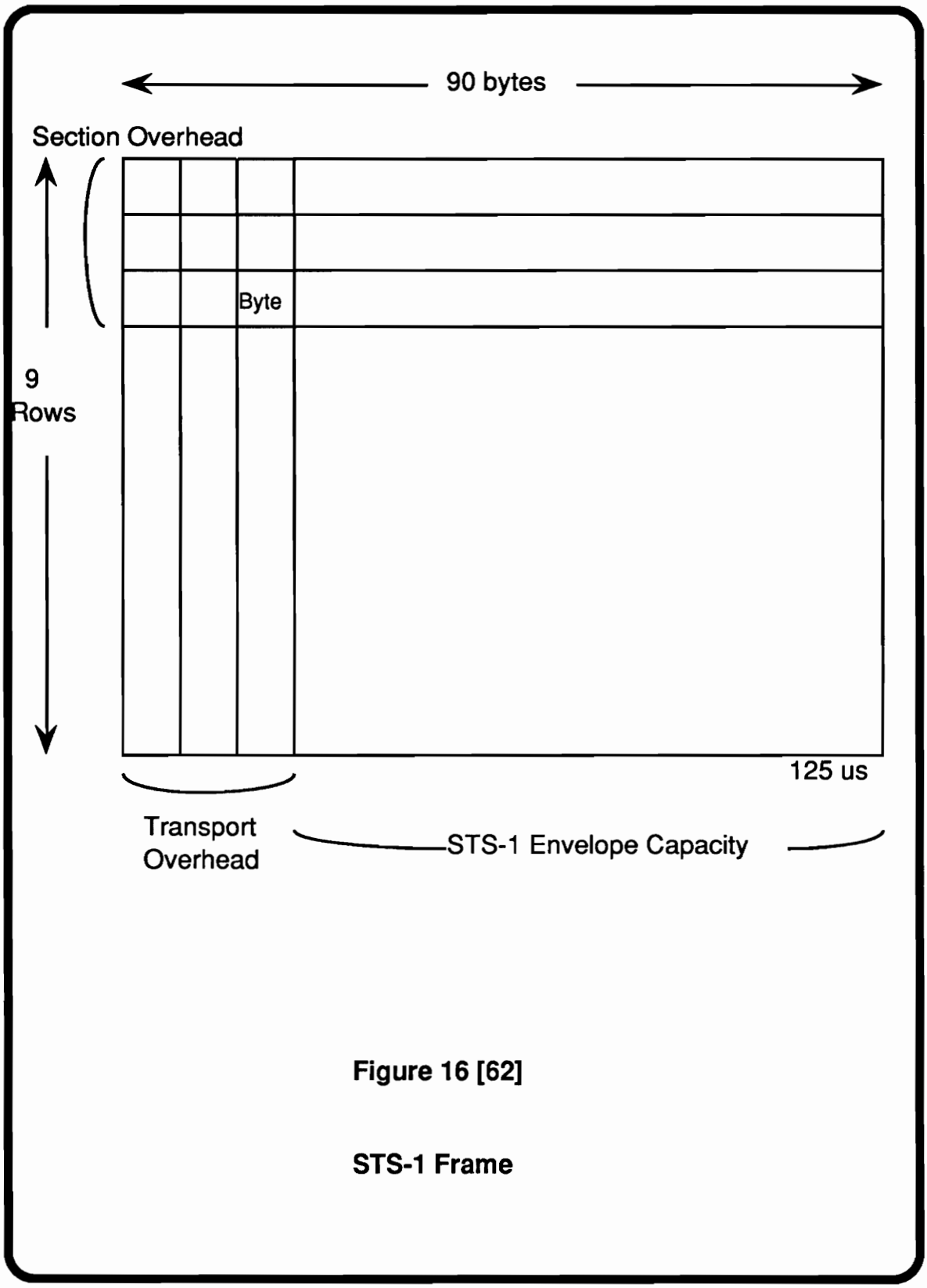

Figure 16 [62]

STS-1 Frame

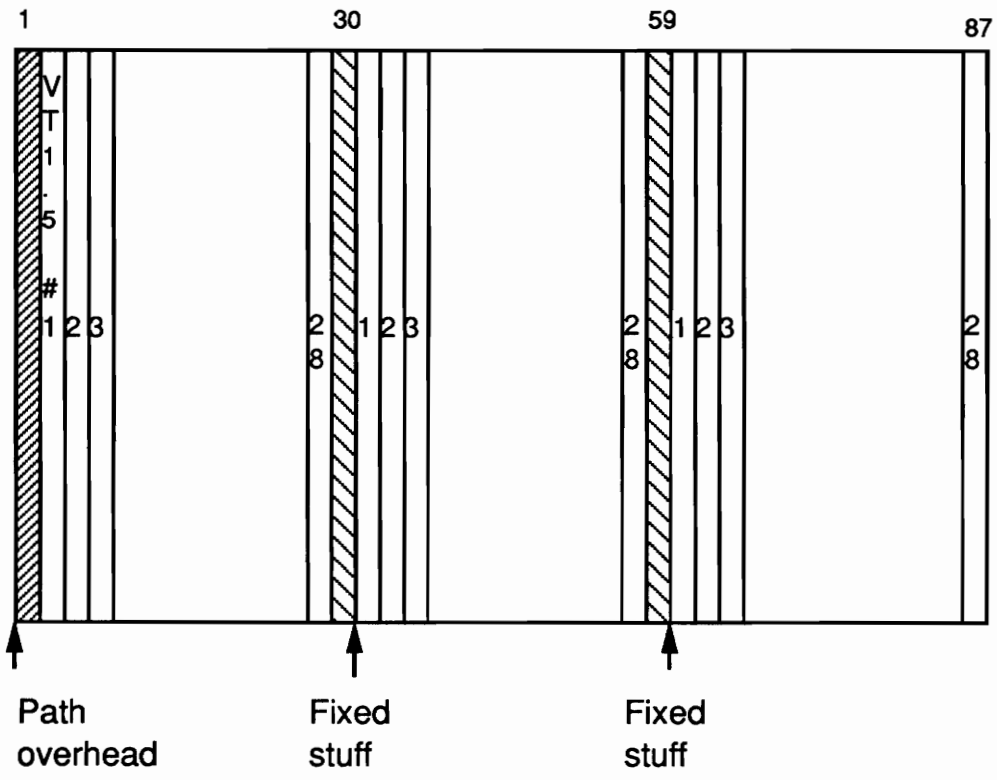

Figure 17 [62]

VT 1.5 Structured STS-1 SPE

7.1.4 Sonet Main Network Elements

The main network elements are the digital cross-connect (DCS), add-drop multiplexer (ADM) and digital switch.

Digital cross-connection includes interfaces at various rates, high speed switching is concerned with the OC-N interface. An incoming OC-N signal is terminated and the individual signals are routed to different outgoing OC-N or lower rate carriers.

The switching characteristics of an add-drop multiplexer is that of extracting and/or adding signals into a passing OC-N.

The digital switch normally follows a cross-connect or an add-drop multiplexer, its main function is pure signal switching in contrast to the DCS and ADM where performance monitoring and protection switching is normally required .

7.1.5 Sonet Layered Overhead

Sonet consists of four layers, from bottom to top they are the physical, section, line and path layers.

The physical layer has no overhead, its main functions are electrical-optical conversions and transmission aspects.

The section layer deals with the transmission of an STS-N frame, regenerators are an example of section terminating equipment. The section overhead occupies the first three rows of the transport overhead.

The line layer deals with the transmission of an STS payload envelope. It includes protection switching. An OC-N to OC-M mux-demux are example of line terminating equipment.

The path layer is responsible for sub STS-1 signal transmission where it performs end to end transmission. DS1-DS3 add drop multiplexer are path terminating equipment.

A layer terminating equipment need not access the overhead of higher layers .

The main overhead bytes are the framing, STS-1 identification, pointers, parity checks, automatic protection switching, path trace, path status, voice channels, data communication bytes and VT overhead .

-The framing bytes occupy the first two bytes of the section overhead and they are used for every STS-1, the sequence is 1111011000101000. These bytes are used as a synchronization reference .

-The STS-1 identification is a section overhead byte that contains a value between 1 and N.

-The pointers determine the start of the envelope payload. The start of data need not be at the start of the envelope capacity rather it can slide as needed. The pointer also includes a concatenation indicator in case of OC-nc signals.

-A parity check byte is found in all three layers. The error check, used for performance monitoring, is a parity one and it is eight-bits interleaved. In the section layer, the parity of the whole STS-N is calculated after scrambling and the result placed in the first STS-1 of the next STS-N before scrambling. Similarly, the line and path error check is calculated over the STS-1 and envelope payload respectively.

-The automatic protection switching (APS) bytes, found in the line overhead includes alarm and failure channels .

-The path trace byte is used for continuous transmission of a 64 byte sequence to the receiving end to justify the connection.

-The path status overhead is for end to end performance monitoring .

-A voice overhead byte is found in both section and line layers, it is used by the network providers as a 64 kbps voice channel among section and line terminating equipments.

-Data communication channels are used for alarm, control, maintenance and administrative signals. They consist of three bytes (192 kbps) in the section layer and nine bytes (596 kbps) in the line layer. These channels as well as the APS channel are still not fully standardized .

-Other main overhead bytes include the VT's overhead which occupies the first byte of the path overhead and includes error check, pointers, path status, VT size..etc.

7.2.0 Optical Technology Implementation in Sonet

Based on the description of the Sonet, one may conclude that the basic functions that are required to be performed at the optical level in order to access an (OC-1,OC-nc or VT) from an OC-N are primarily framing, scrambling and pointer processing. To have a reliable access, the necessary functions are optical error check and optical detection of signal, frame and pointer loss.

7.2.1 Nonlinear FP Logic Implementing Optical Framing

The first required function is optical framing. An optical circuit should observe an incoming Sonet signal and should indicate the detection of the framing sequence. This is a high speed operation where the circuit is required to operate at a rate higher than the transmission one. Based on the technologies described in the previous chapters, the use of nonlinear Fabry-Perot logic and all optical switches is proposed. Below, the performance required from a NLFP in the cascadable structure of the circuit that detects the framing byte (11110110) is analyzed, Figure 18.

The optical splitters are used to provide a copy of every eight bit sequence to the optical logic. This can be done by assuring a distance of a bit period (T_b) between each two. Passive splitters can be attained by insuring that the signal power at each switch is equal to the threshold power P(th) given by equation (2-13).

Since every T_b a new eight bit parallel sequence is incident, then the NLFP relaxation time should be less than the bit period. The first condition concerning the NLFP required performance would be :

$$5\,t_r < T_b \qquad (7\text{-}1)$$

where t_r is the relaxation constant, T_b is the bit period and it is assumed that total relaxation takes 5 time constants.

Observe that NLFP#2 and #3 have inputs that pass through more stages than

others. The number of stages can generally be varied since the same mathematical function can be expressed in several equivalent forms. The available optical logic gates mainly determine the number of stages. If only the NOR function is available than the number of stages are expected to be much larger than if all logic operations are available. The difference in the number of stages is 1 in this case but can be much higher (C) in other circuits. This causes a delay in the arrival of some of the inputs. So, the second requirement is based on the need to have inputs of the same gate incident in within one t_r from each other.

$$C * (T_d) < t_r \qquad (7\text{-}2)$$

where T_d is the NLFP gate delay normally specified as the time interval between the input and output pulses measured at 50% of their high levels.
It is assumed that all NLFP imposes the same delay T_d. With NLFP, T_d is effected by both the propagation in the material and the time difference between the input and the probe.

The output of the circuit is high when the framing byte is the eight bit input, so that this would be the indicator of the start of a frame. The offset between the "1" output and the frame should be much smaller than T_b otherwise the framing circuit itself will cause the misalignment. For the mentioned circuit, the maximum number of stages is three so that

$$3\,T_d \ll T_b \qquad (7\text{-}3)$$

Equations (7-1), (7-2)and (7-3) can be put as:

$$T_d \ll t_r < 0.2\,T_b \qquad (7\text{-}4)$$

At 9.95 Gbps, T_b= 0.1 nsec => t_r < 20 psec

$$\Rightarrow \quad T_d \ll 20 \text{ psec}$$

With $T_d \ll 20$ psec, the NLFP output can be considered to follow the input instantaneously. The NLFP acceptable switching speed t(s) can be approximated by considering the rise and fall times.

t (s) = 0.5 [t (rise) + t (fall)]. For the output pulse to rise and fall within one bit period then the condition is :

$$t(\text{rise}) = t(\text{fall}) < 0.5\, T_b \Rightarrow t(s) < 0.5\, T_b$$

$$\Rightarrow t(s) < 50 \text{ psec}$$

When cascading NLFP, it should be remembered that the probe of a stage becomes the input of the next. The need for the exact probe detuning specifies the probe wavelength, so mainly it is up to the NLFP of the second stage to have an absorption region at that wavelength.

The circuit of Figure 18 does not need realignment since every eight bit sequence is observed, it can provide framing loss indication whenever a "1" output is not observed for a certain specified time. The (1*2) switches were included as a bypass route. Since the framing sequence occupies 2N consecutive bytes, there is no need to observe all 810N bytes of an OC-N frame.

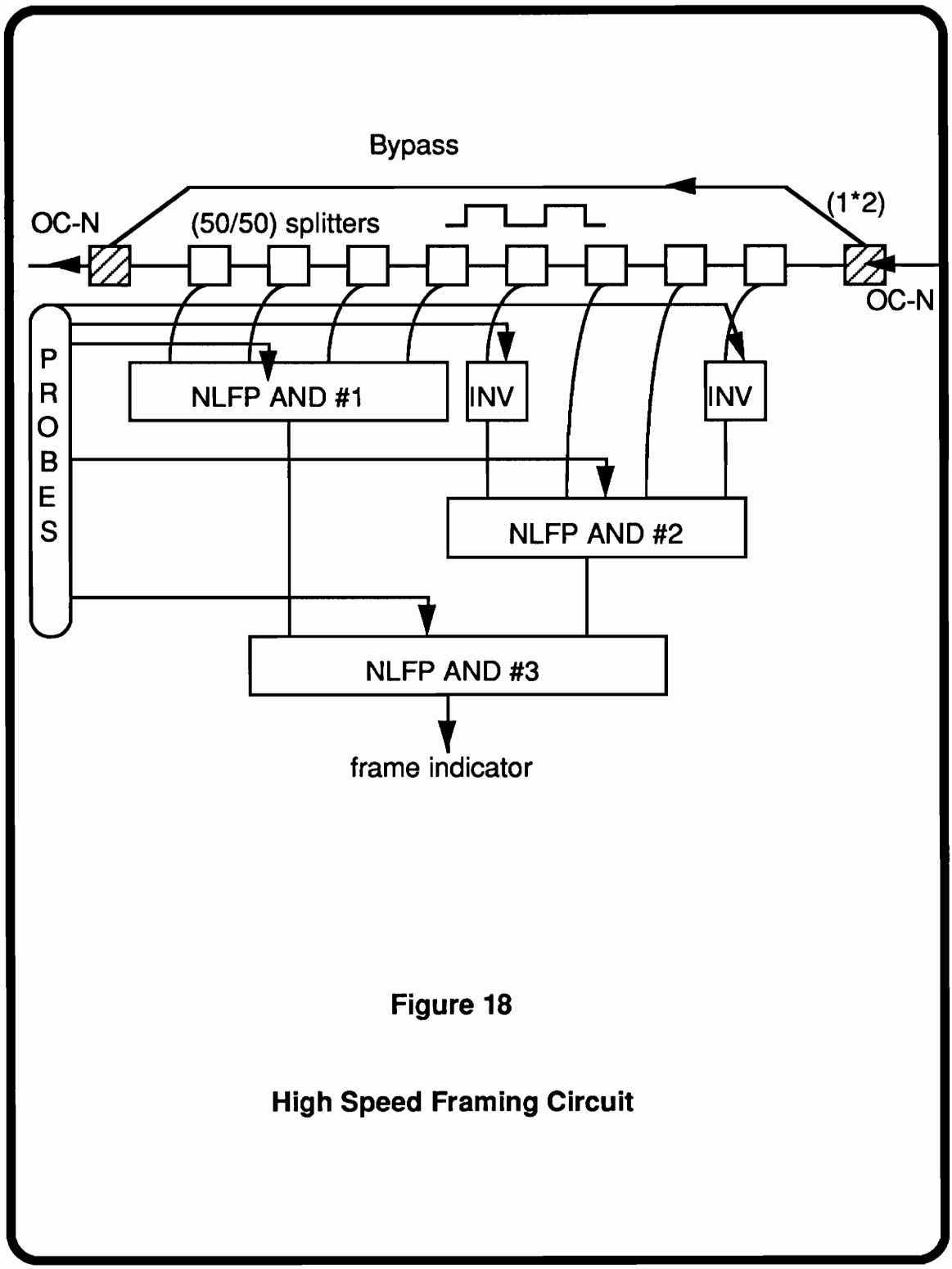

Figure 18

High Speed Framing Circuit

7.2.2 Optical Framing Using Low Speed Logic.

High speed optical logic may not be available or may not be desirable due to large power dissipation or thermal instability. Bit rate logical operation in the previous circuit can be substituted by slower operations at the expense of inability to observe every eight bit sequence and hardware duplication.

A possible architecture is shown in Figure 19 which is based on bit by bit demultiplexing the input stream. The individual bytes are routed to the duplicate circuits in a round fashion. The gain is the minimization of the data rate on each input so that to provide enough switching time for the logical circuit by applying 8 bit input every 24 bit sequence. An individual eight input framing circuit may consist of NLFP or possibly S-SEEDs. If NLFP logic is implemented, then the technology analysis presented in the previous circuit will still hold, the only difference is in equation (7-1) where t_r is multiplied by a factor of 8.

The application disadvantage of this architecture is that it does not observe all sequences and therefore a realignment is needed when an offset occurs. When the output is an all zero sequence, misalignment or loss of frame is indicated. Realignment can be done by blocking certain number of bits in the demultiplexer space division matrix. A bit is blocked when it is not provided with a path to its intended input.

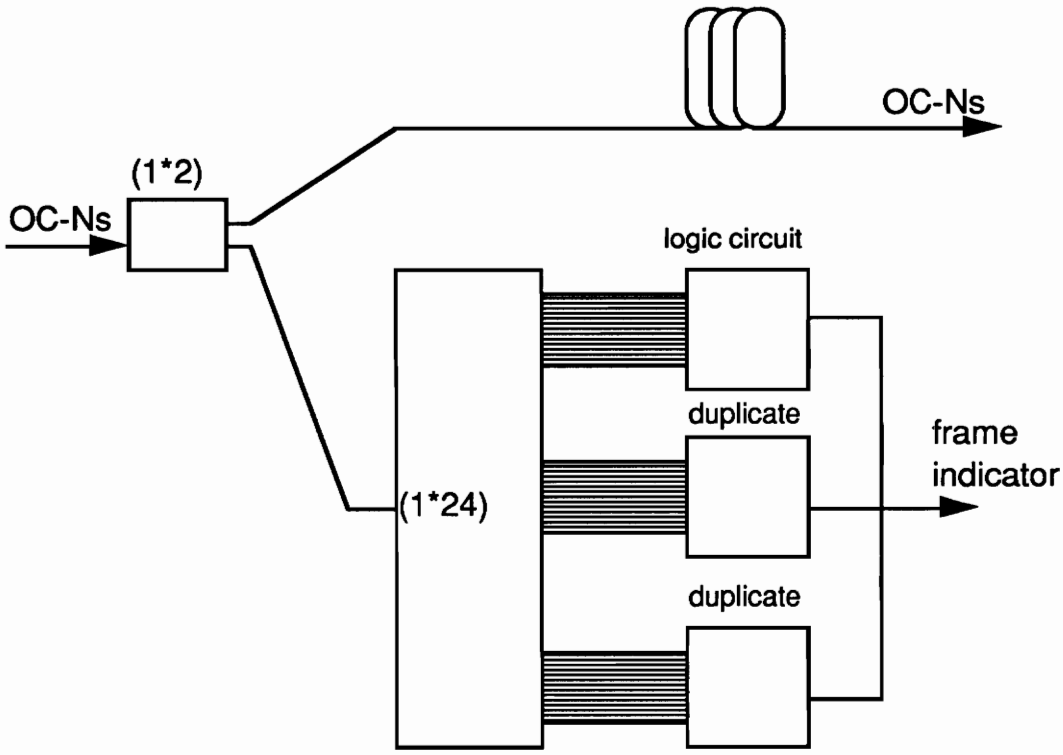

Figure 19

Architecture for Low Speed Framing Circuit

The next following bit occupies that path. For example, if the misalignment is one bit to the right and the blocking is bit by bit, then the supposed 11110110 is first replaced by 11101101 and after six blockings realignment is retained. The input changes as follows (1101101->10110111->0110111->11011110->10111101->01111011-> 11110110). Frame loss is indicated when the realignment process does not recover from an all zero sequence at the frame indicator output.

The (1*2) switch is used as both a passive and active switch. During frame observation, it should work as a 3db splitter where its outputs will form both the original Sonet signal and the frame indicator respectively. For the frame indicator to match the Sonet signal, the latter passes through an optical delay line as shown. The delay value should equal the delay imposed by the logical circuit and as stated earlier, the offset should be much less than a bit period.

7.2.3 The Implementation of Scrambling with Optical Technology

The scrambler specified in the Sonet standard is shown in Figure 20 [62]. To recover the original data, a second scrambling (descrambling) is needed. Scrambling is used in place of encoding. It mainly serves to equalize the transmitted number of "1"s and "0"s and to minimize the occurrence of long sequences of all "1"s or all "0"s. Based on the electrical circuits architecture, an optical translation is discussed. The suitable optical memories according to previous performance analysis (Section 4.1.2) are mainly:

-Fabry-Perot memories (FPM)

-S-SEEDs memories

-Laser diode memory (LDM)

Considering the FPM, two conflicting conditions exist. At any shift, any memory should be relaxed to accept a new data bit and on the other hand it should not be relaxed for it to provide its stored information to the next memory. Similarly laser diodes need to be reset prior to a new input. Resetting them would result in the loss of the bits that should be shifted. The solution is to introduce an architecture that will overcome the optical technology restriction. A possibility is to add an intermediate LD or FP memories in between each two. Shifting would proceed by a first shift to the intermediate memories, followed by resetting or relaxation of the original ones and a second shift to the latters.

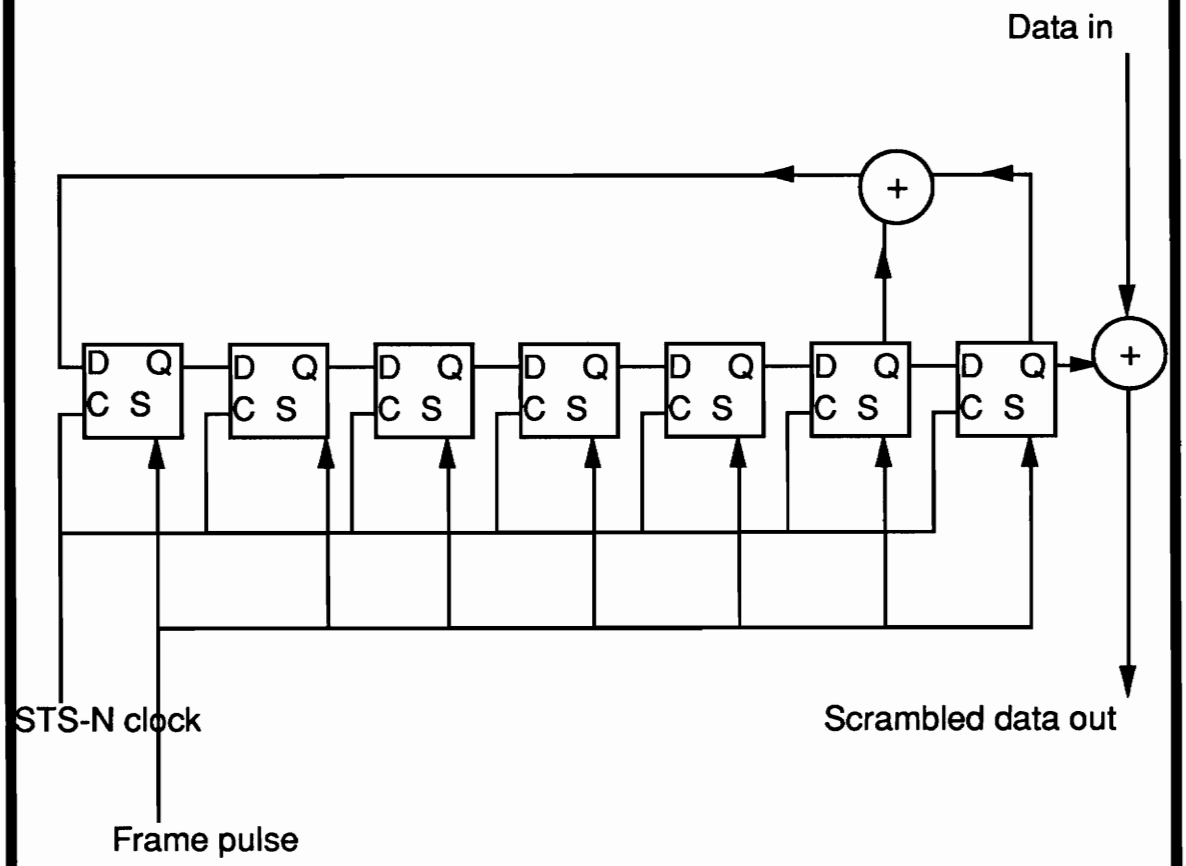

Figure 20 [62]

Frame Synchronous Scrambler

A DQ shift register characteristic is that the Q takes the value of D whenever the clock is applied, normally they are isolated. A LD can have its output isolated from its input by proper bias control, but when operating as a memory the bias source should remain constant as was shown in Figure 9. A suitable architecture is then needed, a possible one is to place an optical switch in between the LDM. The LDM output will always be effected by its input, but now the LDM are isolated. Suitable switches would be the (1*1) LD switches, this allows monolithic integration.

The S-SEED can be operated as a clocked DQ flip-flop. As shown in the literature, the S-SEED operating state is determined by the ratio of its inputs. The second characteristic of S-SEED is that its multiple quantum wells operate in a complementary fashion, when one is transmissive, the other is absorptive. The absorptive MQW corresponds to the higher input. The S-SEED has the capability to operate as a clocked device. This would require low power signals with a large ratio to determine the operating point of the S-SEED. Since the signals are low power and in the pulsed format, they are completely absorbed and do not contribute to any output power. After the MQWs transmission state is set, a clock is applied to both inputs. The clock forms the outputs which are complementary (Q and Qbar). An optical scrambler based on the S-SEED technology is shown in Figure 21.

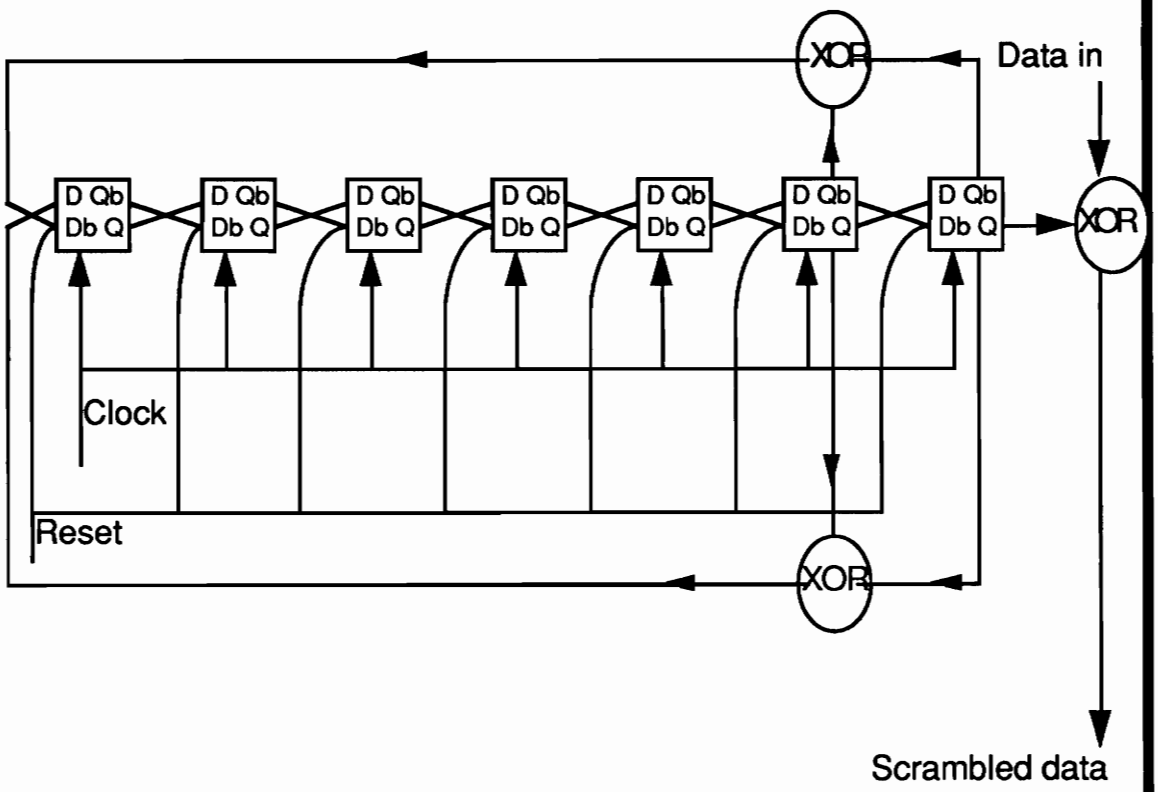

Figure 21

S-SEED Based Optical Scrambler

Since a MQW is absorptive when it has the higher input, then the output of D is Qbar. Consider the interconnection between two shift registers; with (Q1=1,Q1bar=0), then (D2=1 and D2bar=0). Q2s intensity will not be effected since the pulsed D2s had low intensity. When a clock(pump) is applied, this will cause Q2=1 and Q2bar=0. The clock power should be high enough to form Q2and Q2bar but since (Q2,Q2bar) are (D3,D3bar), and it should be low enough for it not to effect (Q3,Q3bar). Another requirement is that the set pulse which is practically connected to all D(bar)s should have a power larger than the clock so that not to have certain unity ratios, case when D=1 and resetting is desired.

The S-SEEDS and LDM have a maximum bit rate of a few Gbps at best. The scrambler is required to provide data at the Sonet signal rate. To overcome this limitation, note that the scrambling is independent of the data, so that several scramblers can be used together. The original scrambler output is 1111111000000100000001000...., for 8 bit interleaved scrambling eight scramblers with outputs 1000.....are needed. Furthermore, the low rate scrambler should be transparent to its non-assigned bits. This can be done by using a NLFP for the XOR gate which have a transmission peak at the data wavelength. When the scrambler has no output, the transmission peak is not shifted and the data is allowed full transmission. As the scrambler output is incident, with the proper detuning it shifts the transmission peak to result in a XOR operation.

Choosing electro-optical memories has the advantage of stable operation compared to all-optical technology. Optical scrambling that uses interleaving to achieve low rate operation. If interleaving can be done at the electrical level, then electrical scrambling is possible even at high rates given the additional complexity of optical to electrical conversion.

7.2.4 Sonet-Based Optical Time-Slot Interchanger

Since Sonet is a time-division multiplexed system, the optical switching technique that will primarily be used is time-division switching. In chapter four, optical time-slot interchangers were discussed and it was found that the most adequate technology at the present time is the parallel delay lines OTSI. These interchangers were demonstrated in the literature with the input data not having any specific format. Sonet OC-N signals are made up of OC-1s, (OC-nc)s, and VTs. Time-division switching should include interchanging OC-1s, (OC-nc)s as well VTs within an OC-1. The unit time-slot of an OC-1 and a VT is a byte whereas it is n bytes for an OC-nc. This is one of the characteristics of the OTSI that is discussed. Given the Sonet format, the parallel reentry and single entry architectures are compared. It is made sure that the proposed device preserves the validity of the signals after interchange and that the number of switches and memories required are kept to a minimum.

An OC-N consists of N OC-1s, so that in general a single byte has N other bytes to possibly interchange with. Yet, some OC-1s will contain VTs. The largest number of VTs in a single OC-1 is 28 VT 1.5, so that a byte belonging to a VT

has an additional 28 interchange choices. For a VT interchange incorporated within an OC-1(OC-nc) interchange, a byte has 28N interchange choices. If the two interchangers are placed in cascade the choice decreases to 28+N. Based on this, the Sonet-based OTSI is proposed be implemented as two structures, one for OC-1(OC-nc) interchange and the other for VT interchange.

7.2.5 OC-1 (OC-nc) Optical Time-Slot Interchanger

The OC interchange is analyzed according to which architecture would be preferred, the single entry or the reentry parallel delays. Normally, the single entry has double the switch count and easier control. I will investigate whether this is still valid in Sonet. The validity of the overhead after interchange is also discussed.

Consider first the reentry configuration. Normally, N delay lines are needed for an N multiplexed signal with constant time slots. When an OC-nc is to be interchanged, it needs a line whose delay is n times the delay of one byte (D_b). Since n is a variable, the required memories adds up to :

N lines	with D_b delay	(n=1)
N/2 lines	with D_{2b} delay	(n=2)
N/3 lines	with D_{3b} delay	(n=3) ...and so on.

where D_{2b} and D_{3b} are the delays of 2 and 3 bytes respectively.

It is a large number which can be decreased by allowing memory sharing between different OC-nc. For instance, a OC-2c can use a D_{3b} 2 times instead

of using D_{2b} 3 times. The above number of memories was based on having OC-Ns formed completely of OC-nc .

In the single entry case, the memories initially had a wide range of delays so that any OC-nc can use them. Therefore generally, no additional memories are needed. The easier control, less signal loss and the introduced increase in the reentry switch count, all favor the implementation of the parallel single entry configuration in the Sonet-based OC-1(OC-nc) optical time-slot interchanger .

In an OC-1 (OC-nc) interchange, the overhead bytes that may be rendered invalid after interchange are the pointers and the OC identifier. The identifier becomes invalid after interchange because an OC-1 keeps its old position number. This is easily solvable through not interchanging the identifier bytes, that is they should keep their own time-slots. These bytes occupies the third N bytes of the frame and thus can be easily identifiable. The pointers indicates the offset of the valid payload data from the start of the payload envelop. In the time-division switching, the offset remains the same and thus the pointers remain valid.

7.2.6 VT Optical Time-Slot Interchanger

This device is proposed to interchange VTs within their corresponding OC-1. The bytes of an OC-1 are N-interleaved in an OC-N, also the VT bytes are interleaved in an OC-1 which results in the bytes of a single VT being uniformly

spread all through an OC-N. The format of a VT1.5 structured OC-1 was shown in Figure 17. A byte has the choice of interchanging with 28 other bytes. The overhead and fixed stuff should remain in their initial positions. The VT time-slot is a byte, but the unit delay is N times the delay of a byte because the bytes of an OC-1 are N-interleaved. A single delay line can thus accommodate up to N bytes. In other words, a VT interchanger for a single OC-1 is capable to interchange the VTs of N OC-1s simultaneously. The question is whether 29 memories for the reentry case are enough. The number 29 is chosen because there are 28 VT and either a fixed stuff or an overhead in each interchange. The answer is approximated by considering two mappings.

{ (0), (30), (59), (1 15), (2 16), (3 17).....(14 28) }
{ (0), (30), (59), (1 28), (2 27), (3 26).....(14 15) }

where (i j) denotes interchange between the ith and jth time-slots. For the i to j interchange,the delay of the memory should be equal to (29-i)+(j-1). The i time slot should wait for the arrival of the remaining time slots belonging to the other VTs and then for it to occupy the outgoing j time slots, it should wait an additional (j-1) time slot.

The first mapping requires 3 D(29Nb), 13 D(42Nb) and 13 D(15Nb).
The second mapping requires 3 D(29Nb), D(1Nb), D(3Nb), D(5Nb) ..... D(27Nb), D(55Nb), D(51Nb), D(47Nb) ..... D(3Nb),
where D(xNb) is the delay of x times N bytes.

Each memory has a delay of Nb, and it can be used in the following byte interchange if the signal needs a delay less than 30Nb. Then the second mapping would have 7 occupied delay lines at the time of arrival of the following set of bytes and 14 occupied for the first mapping. A rough figure is to have 29+14=43 delay lines for the reentry configuration.

Consider the single entry configuration. In general, a set of delay lines from D(2Nb) to D(55Nb) is needed, D(Nb) is dispensable since the 28th byte can never shift to the 0th position occupied by the fixed stuff and overhead. Considering the above mappings, it is observed that some delay lines (42Nb,15Nb..) are used by 13 time slots belonging to the same OC-1. In case the VT interchange for all OC-1s have the same mapping, then there will be 13N time slots in the 15Nb delay line. This is below its full capacity, nevertheless some duplications are necessary for the memories with a short delay.

Since each delay line in both configurations contains a large number of time slots, the primary concern is that of the control complexity rather than the memory count savings (43 versus 53+duplicates). The reentry case is not suitable for VT interchange because there is a considerable probability of a signal hit especially when a delay line is accommodating a number of time slots close to its capacity. A signal hit is the case when a time slot is trying to enter the memory for the first time and another time slot needs to reenter. The reentry switch can either be configured in the bar or cross state and hence one of the time slots will be hit.

7.2.7 General Application of Optical Technology

The emphasis in the application of optical switching in Sonet was on optical logic and optical time division switching. This is primarily because Sonet employs time-division multiplexing. As for the application of optical space and frequency switches described in this survey, one may conclude the following:

Optical space switches applications depend mainly on the speed offered by these devices. Polarization dependency and the other performance parameters are also a factor, but if the switch cannot operate at very high speeds, then its application is limited.

Thermo-optic switches have switching speeds in the millisecond range, their possible application is in very slow switching functions such as facility switching.

Electro-optic or carrier injection technology have considerable switching speeds. They may exceed 10 GHZ switching rates indicated in Section 2.3.2, but in general the (1-10) GHZ range is a representative figure. These technologies are more advanced than all-optical switches and especially in the implementation of switching matrices. What is required is probably for the Sonet format to provide "guard bands", so that these switches have enough time to rise and fall without losing valid data. The following approaches are proposed:

-Dedicate some OC-1s or OC-nc for guard bands. Since Sonet byte multiplexes its individual channels, these guard bands will appear all through

the signal with unit length of one byte or n bytes.

-A less costly method is to dedicate VTs as guard bands .

-For either choice , apply time slot interchange to place the guard bands on both sides of the intended channel or channels to be switched .

-The guard band indicator may be one of the unused bytes in the overhead

The application of wavelength multiplexing along with optical switching depends on the realization of wavelength independent optical switches. Nevertheless, wavelength shifting devices are required to perform minor functions such as detuning in the described FP optical logic. The preferred technology is the tunable local oscillators since they provide nanosecond tuning speeds in comparison to the msec values of acousto-optics.

As for the Sonet applications required for switching and maintaining the network, a whole set of them was neglected. This is because the optical circuits required would probably be similar to the described ones. Briefly, error checking can be best realized by NLFP which provides the XOR function in a single gate . The parity calculation needs a feedback, this can be realized by an optical delay line. Signal loss needs a high speed combinational circuit that operates at the line rate and thus is similar to the high speed framing one. The signal pointer needs to be processed primarily to determine if the signal is an OC-1 or an OC-nc. The offset is not important since the valid payload can be extracted from the payload envelop at low rates. Also, the data communication channels and the path performance signals are kbps channels that are processed by the terminating equipments.

8.0 SUMMARY

This survey covered optical space, time and frequency division switching and integrated optical logic. Sonet based applications consisting of optical logic circuits and a time-division switch were discussed.

Optical switches are mainly based on three principles which are mode coupling, mode interference and reflection from a refractive index barrier. The technologies used are primarily electro-optics, carrier injection, thermo-optics and all-optical. Electro-optics shows polarization dependent switching which can be countered using several approaches. Thermo-optics switches are slow having switching speeds in the millisecond range. Electro-optical and carrier injection speed are normally in the nanosecond range. Only all-optical technology is able to reach sub-picosecond switching times.

Optical switching matrices are made-up of individual optical switches. Their sizes are primarily limited by the individual switch crosstalk and attenuation. The "dilation" technique overcomes the crosstalk limitation and (1*1) laser diode amplifier switches can be used to build lossless switching matrices. To overcome the small substrate sizes, the "reflection" technique increases the switch integration level.

Optical memories are mainly based on magneto-optics, electron-trapping or optical bistability. For the optical time-slot interchange application, the

suitable technology is optical delay line which is not a general purpose memory. An optical time-slot interchanger can have different configurations based on single entry or reentry, parallel or series delay lines.

Optical wavelength division switching needs optical wavelength multiplexers, demultiplexers and shifters. Wavelength shifting can primarily be done by acousto-optics or by optical to electrical conversion and retransmission. Acousto-optic switches have millisecond tuning speeds in contrast to nanosecond switching for local oscillators.

Integrated optical logic main components are the Fabry-Perot resonator and the self-electro-optic effect device (SEED). The FP nonlinear logic is capable of performing all logic operations at THZ rates. The SEED technology offers a higher degree of stability, but its speed is comparable to that of electronics.

As an application to the above survey, optical combinational and sequential circuits were discussed as well as a Sonet based time-division switch. This included high speed framing circuit, architecture that allows framing with lower speed optical logic, S-SEED based optical scrambler, an optical carrier time-slot interchanger and a virtual tributary time-slot interchanger.

REFERENCES

The references marked with * can be found in the book: "Photonic Switching" edited by H.S. HINTON and J.E. MIDWINTER, IEEE Press, 1990. Those marked with ** can be found in the book "Photonic Switching" edited by T.K. GUSTAFSON and P.W. SMITH,1987.

[1]* KOGELNIK, H., and SCHMIDT, R.V.: 'Switched directional couplers with alternating Δß', *IEEE Journal of Quantum Electronics*, Vol. QE-12, No. 7, pp. 396-401, July 1976.

[2] FORBER, R.A., and MAROM, E.: 'Symmetric directional coupler switches', *IEEE Journal of Quantum Electronics*, Vol. QE-22, No. 6, pp. 911-919, June 1986.

[3]* SCHMIDT, R.V., and ALFERNESS, R.C.: 'Directional coupler switches, modulators, and filters using alternating Δß techniques', *IEEE Trans. Circuits Syst.*, Vol. CAS-26, pp.1099-1108, December 1979.

[4] FRIBERG, S.R., SILBERBERG, Y., OLIVER, M.K., ANDRESCO, M.J., SAIFI, M.A., and SMITH, P.W.: 'Ultrafast all-optical switching in a dual-core fiber nonlinear coupler', *Applied Physics Letters*, Vol. 51, No. 15, October 1987.

[5]* FRIBERG, S.R., WEINER, A.W., SILBERBERG, Y., SFEZ, B.G., and

SMITH, P.S.: 'Femtosecond switching in a dual-core-fiber nonlinear coupler', *Optics Letters*, Vol. 13, No. 10, pp. 904-906, October 1988.

[6] TOMLINSSON, W.J., STOLEN, R.H., and SHANK, C.V.: 'Compression of optical pulses chirped by self-phase modulators in fibers', *Journal of the Optical Society of America*, Vol. 1, No. 2, pp. 139-149, April 1984.

[7] PERSONICK, S.D.: 'Update on Photonic Switching', *International Switching Symposium,* Vol. 4, paper C12.4, pp. 1009-1014, 1987.

[8]** PATON, C.R., SMITH, S.D., and WALKER, A.C.: 'An all-optical switch for signal routing between fibers, *Proceedings of the first topical meeting on photonic switching*, pp. 59-62, March 1987.

[9]** CHELLI, H., NIEPCERON, A., PARAIRE, N., KOTER, A., SAUER, H., CARTON, M., and LAVALI, S.: 'fast all-optical switching in a silicon-on saffire waveguide', *Proceedings of the first topical meeting on photonic switching*, pp. 129-131, March 1987.

[10]* NEYER, A.: 'Electro-optic X-switch using single-mode Ti:LibO3 Channel waveguides', *Electronics Letters,* Vol. 19, No. 14, pp. 553-554, July 1983.

[11] ISHIDA, K., NAKAMURA, H., MATSUMURA, H., KADOI, T., INOUE, H.: 'InGaAsP/InP optical switches using carrier induced refractive index change', *Applied Physics Letters*, Vol. 50, No. 3, pp 141-142, January 1987.

[12] SCHMITT, H.J.: 'Magneto-optic devices', *The International Society of Optical Engineering*, SPIE Vol. 1274, pp. 208-218, 1990.

[13]** TOROK, E.J., KRAWCSZAK, J.A., NELSON, G.L., FRITZ, B.S., HARVEY, W.A.,and HEWITT, F.G.: 'Photonic switching with stripe domains', *Proceedings of the first topical meeting on photonic switching*, pp. 46-49, March 1987.

[14] TSAI, C.S., KIM, B., EL-AKKARI, F.R.: 'Optical channel waveguide switch and coupler using total internal reflection', *IEEE Journal of Quantum Electronics*, Vol. QE-14, No. 7, pp. 513-517, July 1978.

[15] YANAGAWA, H., UEKI, K., and KAMATA, Y.: 'Polarization and wavelength insensitive guided-wave optical switch with semiconductor Y-junction', *Journal of Lightwave Technology*, Vol. 8, No. 8, pp. 1192-1197, August 1990.

[16] MENDOZA-ALVAREZ, J.G., COLDREN, L.A., ALPING, A., YAN, R.H., HAUSKEN, T., LEE, K., and PEDROHI, K.: 'Analysis of depletion edge translation lightwave modulation', *Journal of Lightwave technology,* Vol. 6, No. 6, pp. 793-807, June 1988.

[17] DIEMEER, M.B.J., BRONS, J.J., and TROMMEL, E.S.: 'Polymeric optical waveguide switch using the thermooptic effect', *Journal of Lightwave Technology,* Vol. 7, No 3, March 1989.

[18] SCHMIDT, R.V., and KOGELNIK, H.: 'Electro-optically switched coupler with stepped Δß reversed using Ti diffused LiNbO3 waveguides', *Applied Physics Letters*, Vol. 28, No. 9, pp. 503-506, 1976.

[19] THYLEN, L.: 'Devices for Photonic Switching', *Proceedings of the first topical meeting on photonic switching*, pp. 101-107, 1987.

[20]* RAMASWAMY, V., DIVINO, M.D., and STANDLEY, R.D.: 'Balanced bridge modulator switch using Ti diffused LiNbO3 strip waveguides', *Applied Physics Letters*, Vol. 32, No. 10, pp 644-646, May 1978.

[21] HARUNA, M., KOYAMA, J.: 'Thermooptic deflection and switching in glass', *Applied Optics*, Vol. 21, No. 9, pp. 3461-3465, October 1982.

[22] Gustavsson, M., Thylen, L., and Djupsjoback, A.:'Traveling wave semiconductor laser amplifiers for simultaneous amplification and detection: systems experiment', *Proceedings of the first topical meeting on photonic switching*, pp. 74-76, 1987.

[23]* ALFERNESS, R.C.: 'Polarization-independent optical directional couplers switch using weighted coupling', *Applied Physics Letters*, Vol. 35, No.10, pp. 748-750, November 1979.

[24] TAMIR, T.(Editor): 'Guided-wave optoelectronics', Chapter 4, Section 7,

pp. 198-201, 1988.

[25] NORDIN, R.A., and RATAJACK, M.T.: 'Characteristics of high-speed electrodes for LiNbO3 electro-optic switch arrays', *Proceedings of the first topical meeting on photonic switching,* pp. 111-116, 1987.

[26] HARVEY, G.T.: 'The photorefractive effect in directional coupler and Mach-Zehnder LiNbO3 optical modulators at 1.3um', *Journal of Lightwave Technology*, Vol. 6, pp. 872-876, 1988.

[27] HINTON, H.S.: 'A Nonblocking Optical Interconnection Network Using Directional Couplers', *Globecom ,* paper. 26.5, pp. 885-888, 1984.

[28]* PADMANABHAN, K., and NETRVALI, A.N.: 'Dilated networks for photonic switching', *IEEE Trans. on Comm.*, Vol. 35, No. 12, pp. 1357-1365, December 1987.

[29] MATSUNAGA, T., KIKUCHI, K., and IKEDA, M.: 'Optical space division switching using laser diode optical switches', *International Switching Symposion,* Vol. 4, paper C12.3, pp. 1004-1008, 1987.

[30]* EVANKOW, J.D., and THOMPSON, R.A.: 'Photonic switching modules designed with laser diode amplifiers', *IEEE J. Sel Areas Comm,* Vol. 6, No. 7, pp. 1087-1095, August 1988.

[31]* SPANKE, R.A.: 'Architectures for large nonblocking optical space switches', *IEEE Journal of Quantum Electron*, Vol. 22, No. 6, pp. 964-967, June 1986.

[32] MURPHY, T.O., HERNANDEZ-GILL, F., VSELKA, J.J., and KROTKY, S.K.: 'Reduced waveguide intersection losses for large tree-structured Ti:LiNbO3 switch arrays', *Proceedings of the first topical meeting on photonic switching*, pp. 117-120, 1987.

[33] KOAI, K.T., and LIU, P.: 'Modeling of Ti:LiNbO3 waveguide devices: part 2, S-shaped channel waveguide bends', *Journal of Lightwave Technology*, Vol. 7, No. 7, pp. 1016-1021, July 1989.

[34] NEYER, A.: 'Integrated-optic devices in Lithium Niobate technology and applications', *The International Society of Optical Engineering*, SPIE Vol. 1274, pp. 2-17, 1990.

[35] LEVENE, M.L.: 'High performance optical disk recorder -preliminary test results and spaceflight model projections', *The International Society of Optical Engineering*, SPIE Vol. 1316, pp. 48-52, 1990.

[36] LINDMAYER, J.: 'Electron trapping for mass data storage memory', *The International Society of Optical Engineering*, SPIE Vol. 1401, pp. 103-110, October 1990.

[37]* JEWELL, J.L., SCHERER, A., McCALL, S.L., GOSSARD, A.C., and ENGLISH, J.H.: 'GaAs-AlGaAs monolithic microresonator arrays', *Applied Physics Letters*, Vol. 51, No. 2, pp. 94-96, July 1987.

[38]* MILLER, D.A.B., CHEMLA, D.S., DAMEN, T.C., BURUSS, C.A., GOSSARD, A.C., and WIEGMANN, W.: 'The quantum well self-electro-optic effect devices: optoelectronicl bistability and oscillation, and self-linearized modulation', *IEEE Journal of Quantum Electron*, Vol. 21, No. 9, pp. 1462-1476, September 1985.

[39]* SUZUKI, S., TERAKADO, T., KOMATSU, K., NAGASHIMA, K., SUZUKI, A., and KONDO, M.: 'An experiment on high-speed optical time-division switching', *Journal of Lightwave Technology,* Vol. 4, No. 7, pp 894-899, July 1986.

[40] THOMPSON, R.A.: 'Optimizing photonic variable-integer-delay circuits', FD4-1.

[41] MAGDICH, L.N., and MOLCHANOV, V.Y.: 'Acousto-optic Devices and their Applications', chapter 1, PP. 1-5, 1989.

[42] KINGSTON, R.H., BECKER, R.A., and LEONBERGER, F.J.: 'Broadband guided-wave optical frequency translator using an electro-optical Bragg array', *Applied Physics Letters*, Vol. 42, No. 9, pp. 759- 761, May 1983.

[43] CHENG, Z.Y., and TSAI, C.H.: 'A novel integrated acousto-optic frequency shifter', *Journal of Lightwave Technology*, Vol. 7, No. 10, pp. 1575-1580, October 1989.

[44] KOBRINSKI, H., VECCHI, M.P., CHAPURAN, T.E., GEORGES, J.B., ZAH, C.E., CANEAU, C., MENOCAL, S.G., LIN, P.S.D., GOZDZ, A.S., and FAVIRE, F.J.: 'Simultaneous fast wavelength switching and intensity modulation using a tunable DBR laser', *IEEE Photonics Technology Letters,* Vol. 2, No. 2, pp. 139-142, February 1990.

[45] KOBAYASHI, K., and MITO, I.: 'Single frequency and tunable laser diodes', *Journal of lightwave Technology*, Vol. 6, No. 11, pp. 1623-1633, November 1988.

[46] GOTO, N., and MIYAKASI, Y.: 'Wavelength-multiplexed optical switching system using acousto-optic switches', *Globecom,* paper 33.7, pp. 1305-1309,1987.

[47] ISHIO, H., MINOWA, J., and NOSU, K.: 'Review and status of wavelength division multiplexing technology and its applications', *Journal of Lightwave Technology*, Vol. 2, No. 4, pp. 448-461, August 1984.

[48] VERBEEK, B.H., HENRY, C.H., OLSSON, N.A., ORLOWSKY, K.J., KAZARINOV, R.F., and JOHNSON, B.H.: 'Integrated four-channel Mach-Zehnder multiplexer demultiplexer fabricated with phosphorous doped SiO2

waveguides on Si', *Journal of Lightwave Technology,* Vol. 6, No. 6, pp. 1011-1015, June 1988.

[49] ROTTMANN, F., NEYER, A., MEVENKAMP, W., and VOGES, E.: 'Integrated-optic wavelength multiplexers on lithium niobate based on two-mode interference', *Journal of Lightwave Technology,* Vol. 6, No. 6, pp. 946-952, June 1988.

[50] HENRY, C.H., KAZARINOV, R.F., SHANI, Y., KISTLER, R.C., POL, V., and ORLOWSKY, K.J.: 'Four channel wavelength division multiplexers and bandpass filters based on elliptical Bragg reflectors', *Journal of Lightwave Technology,* Vol. 8, No. 5, pp. 748-755, May 1990.

[51] MALLINSON, S.R.: 'Wavelength selective filters for single mode fiber WDM systems using Fabry-Perot interferometers', *Applied Optics,* Vol. 26, No. 3, pp.430-436, February 1987.

[52] MAEDA, M.W., SESSA, W.B., WAY, W.I., YI-YAN, A., CURTIS, L., SPICER, R., and LAMING, R.I.: 'The effect of four-wave mixing in fibers on optical frequency-division multiplexed systems', *Journal of Lightwave Technology*, Vol. 8, No. 9, pp. 1402-1407, September 1990.

[53]* MILLER, D.A.B., CHEMLA, D.S., DAMEN, T.C., GOSSARD, A.C., WIEGMANN, W., WOOD, T.H., and BURRUS, C.A.: 'Novel hybrid optically bistable switch: the quantum well self-electro-optic effect device', *Applied*

Physics Letters, Vol. 45, No. 1, pp. 13-15, July 1984.

[54]* SMITH, S.D.: 'Optical bistability, photonic logic, and optical computation', *Applied ptics*, Vol. 25, No. 10, pp. 1550-1564, May 1986.

[55]* JEWELL, J.L., RUSHFORD, M.C., GIBBS, H.: 'Use of a single nonlinear Fabry-Perot etalon as optical logic gates, Apllied Physics Letters, Vol. 44, No.2, pp. 172-174, January 1984.

[56] JEWELL, J.L., LEE, Y.H., WARREN, M., GIBBS, H.M., PEYGHAMBARIAN, N., GOSSARD, A.C., and WIEGMANN, W.: '3pJ, 82MHZ optical logic gates in a room temperature GaAs-AlGaAs multiple quantum well etalon', *Applied Physics Letters,* Vol. 46, No. 10, pp. 918-920, 19

[57]* SMITH, P.W.: 'On the physical limits of digital optical switching and logic elements', *Bell System Technical Journal,* Vol. 61, No. 8, pp. 1975-1993, October 1982.

[58] LENTINE, A.L., HINTON, H.S., MILLER, D.A.B., HENRY, J.E., CUNNINGHAM, J.E., and CHIROVSKY, L.M.F.: 'Symmetric self-electro-optic effect device: optical set-reset latch', *Aplied Physics Letters,* Vol. 52, No. 17, pp. 1419-1421, April 1988.

[59] LEE, Y.H., GIBBS, H.M., JEWELL, J.L., DUFFY, J.F., VENKAKSAN, T., GOSSARD, A.C., WIEGMANN, W., ENGLISH, J.H.: 'Speed and effectiveness of

windowless GaAs etalons as optical logic gates', *Applied Physics Letters*, Vol. 49, No. 9, pp. 486-488, September 1986.

[60] WALTHER, M., EBELING, K.J.: 'Switching characteristics of SEEDs with integrated Fabry-Perot resonator', *The International Society of Optical Engineering,* SPIE Vol. 1280, pp. 109-114, March 1990.

[61] Lightwave Magazine, p. 35, April 1991.

[62] Bellcore Technical Reference: 'Synchronous Optical Network (SONET) Transport Systems : Common Generic Criteria', TR-TSY-000253, Issue 1, September 1989.

VITA

Philip Tohme was born in Beirut, Lebanon. He took his bachelor degree in electrical engineering from the American University of Beirut. He then traveled to the United States to get his masters degree from Virginia Polytechnic Institute and State University. He worked as a summer student both with Getco Telecom,Lebanon and Alcatel Cable Systems, Virginia. Right now, he is looking for employment.

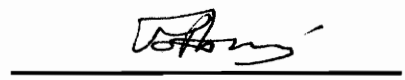

Philip Edward Tohme